# Backbone free energy estimator applied to viral glycoproteins

Robert C. Penner<sup>1,2</sup>

<sup>1</sup>Institut des Hautes Études Scientifiques, Le Bois-Marie, 35 route de Chartres, 91440 Bures-sur-Yvette, France <sup>2</sup>Mathematics Department, University of California at Los Angeles, Los Angeles, CA 90095, USA

Abstract: Earlier analysis of the Protein Data Bank derived the distribution of rotations from the plane of a protein hydrogen bond donor peptide group to the plane of its acceptor peptide group. The quasi Boltzmann formalism of Pohl-Finkelstein is employed to estimate free energies of protein elements with these hydrogen bonds pinpointing residues with high propensity for conformational change. This is applied to viral glycoproteins as well as capsids, where the 90th-plus percentiles of free energies determine residues that correlate well with viral fusion peptides and other functional domains in known cases and thus provide a novel method for predicting these sites of importance as antiviral drug or vaccine targets in general. The method is implemented at https://bion-server.au.dk/hbonds/ from an uploaded Protein Data Bank file.

**Keywords**: Proteins, Backbone Hydrogen Bonds, Backbone Free Energy, Viral Glycoproteins, Antiviral Vaccine/Drug Targets

# Introduction

The viral lifecycle [1, 2] involves several activities: adsorption, entry, uncoating, transcription/mRNA production, synthesis of viral components, virion assembly and release. Here are studied the first two stages which might be characterized as recognition/binding [3]-[5] with the host cell and subsequent fusion/penetration [6]-[11] of cell or endosomal membrane. This is typically accompanied by dramatic reconformation in order to fashion characteristic fusion/penetration motifs. A general method is presented to predict such residues of high conformational activity from 3d structure.

Viruses can be enveloped in a lipid bilayer, non-enveloped and contained in a protein capsid, or may be enveloped for only part of their lifecycle. Enveloped viruses are best understood, and their envelopes support glycoproteins [12, 13] orchestrating both recognition/binding and fusion/penetration. With this case in mind, one might rightly think of the glycoprotein as a mechanical device primed for reconformation with appropriate stimuli.

The free energy of a protein feature provides a measure of its stability [14]. While most features of a protein must have low free energy in order to stabilize the structure, there are also energy defects as reflected by *exotic* features, as they shall be called here, with high free energy. Such exotic features occur only rather rarely and may arise for functional reasons.

Such defect may be tolerated, preserved by evolution and compensated by other low free energy regions, because it is required for protein function, especially in cases when the function consists of conformational change: an unstable feature will more likely change conformation in a biologically reasonable time while a stable structure without defects would likely take too long to reorganize. Receptor binding and fusion peptides are just such cases as their function is connected with conformational change.

These considerations lead to the scrutiny of exotic features of viral glycoproteins undertaken

here. This regime is probed by applying the quasi Boltzmann formalism, observed by Pohl [15] and explained by Finkelstein et al. [16, 17], to the distribution of hydrogen bond geometry compiled from an unbiased subset of the Protein Data Bank (PDB) [18]. Hydrogen bonds of a subject protein might be analyzed and free energy differences of corresponding features computed via relative densities in the distribution with residues determined where conformational change is likely, which it has been argued should comprise significant functional domains.

In multiple cases where these regions have been determined, the method discussed here succeeds in accurately identifying them. This therefore offers the prospect of prediction in cases where they have not been determined.

After first reviewing background material, namely the application of the PDB-derived distribution using the quasi Boltzmann formalism, several viral glycoproteins are studied in detail to establish credibility of the method. The bulk of this manuscript is a table for a multitude of viral glycoproteins containing those residues involved in features with high free energy hydrogen bonds between peptide groups, as well as for several non-enveloped viral capsids.

This table of residues offers prediction of recognition/binding, fusion/penetration and other functional sites for viruses as argued above. At least it provides potential targets for mutational knockdown of functional domains. These residues moreover provide appealing targets for drugs or vaccines not only because their obstruction should interrupt function but also because exotic peptides by their very nature occur rarely in the host organism therefore minimizing the likelihood of side-effects; it is worth noting, however, that there are no human fusion peptides in the PDB at this time for example.

# **Background**

As introduced and developed in [19] and illustrated in Figure 1, two peptide groups sharing a backbone hydrogen bond (BHB) ordered from donor to acceptor provide a unique rotation

of 3d space as determined by an axis of rotation and an amount of rotation about it. The "collection of all 3d rotations" is abbreviated simply by the group SO(3) following mathematical traditions. Mathematics furthermore endows SO(3) itself with intrinsic notions of distance, angle and volume.

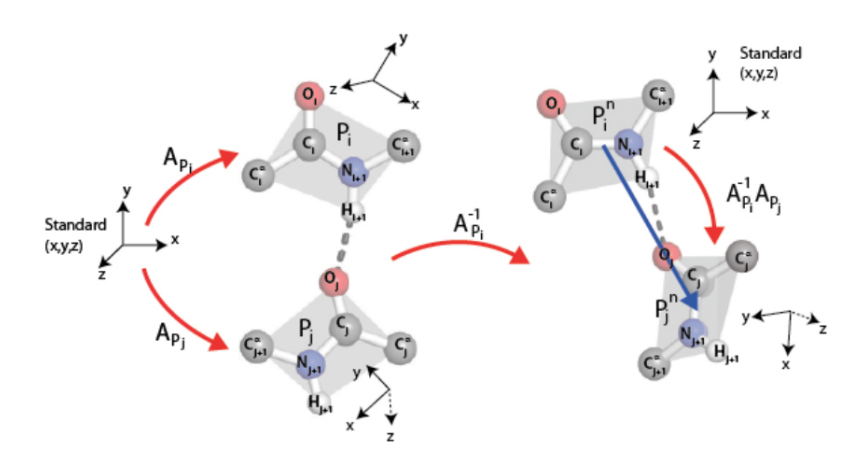


Figure 1: On the left are depicted two peptide groups  $P_i$ ,  $P_j$  participating in a hydrogen bond with donor  $P_i$  and acceptor  $P_j$ . The planes of these peptide groups are illustrated in grey. There is a unique 3d rotation  $A_{P_i}$  carrying the (oriented) xz plane to the grey plane for  $P_i$  and sending the positive x-axis to the ray  $\overrightarrow{C_iN_{i+1}}$ , and likewise  $A_{P_j}$  for  $P_j$ . The composition  $A_{P_i}^{-1}A_{P_j}$  illustrated on the right is the rotation in SO(3) associated to the pair  $P_i$ ,  $P_j$ . See SM for details.

Upon choosing an unbiased representative subset of PDB called HQ60 for high-quality 3d structures with 60% and below homology identity which is culled from PDB using PISCES [20], one might study the histogram of all BHBs that occur, some 1166165 in number, cf. Supplementary Material (SM) for more detail. The results reveal that the rotations that occur for these BHBs (or as abbreviated simply the BHBs themselves) in HQ60 occupy only about 32.5% of the volume of SO(3); this distribution in SO(3) is depicted in Figure 2.

As explained in [14, Lecture 16], specific features of proteins obey a so-called *quasi Boltz-mann* law in the sense that feature occurrence is proportional to  $\exp(-F/kT_C)$ , where F is the free energy of the feature, k is the Boltzmann constant and  $T_C$  is an effective temperature, the

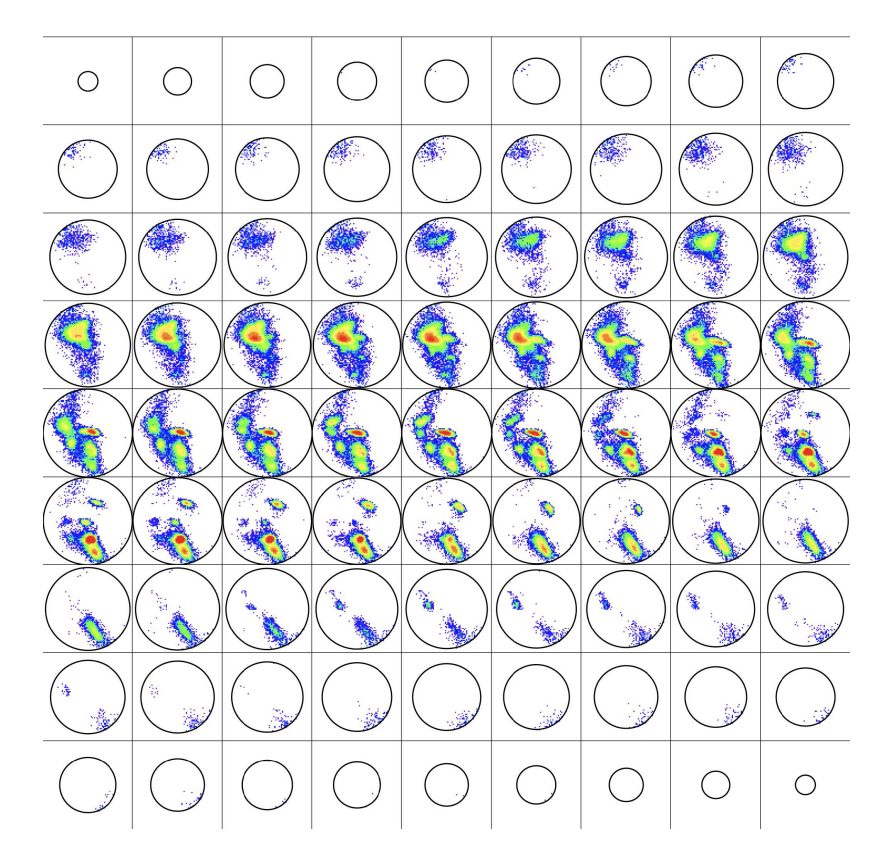


Figure 2: As explained in SM, SO(3) may be visualized as a 3d ball of radius  $\pi$ . Presented here are 81 horizontal slices of the histogram of BHBs in HQ60 in this ball from North to South pole colored by population density from [19], where the R-Y-G-B color is linear in the density ranging from 19000 to 1.

conformational temperature of approximately 350 degrees Kelvin, roughly the melting temperature of protein, with  $kT_C$  about 0.7 kcal/mole at room temperature, compared to kT=0.6 kcal/mole with T the temperature of about 300 in degrees Kelvin. These are not Boltzmann statistics in the usual sense of a particle visiting states with a probability proportional to the energy divided by -kT, but rather reflect the statistics of words in the alphabet of amino acids which stabilize proteins with the particular feature, cf. [14, 16, 17].

More explicitly, consider again the distribution on the 3d ball SO(3) illustrated in Figure 2. SO(3) is dissected into roughly a quarter million *boxes* of small equal Euclidean volume, and the *density* d(p) at any BHB rotation p in SO(3) is the number of points of the distribution in

the box containing p divided by the SO(3) volume of the box. Thus is the density determined as a function on SO(3) that takes a constant value on each box. There is a point m in SO(3) of highest density d(m)=19000 at the rotation unsurprisingly corresponding to the ideal (right)  $\alpha$  helix. To fix an overall scale, the quantity

$$\Pi(p) = \ln(d(m)/d(p))$$

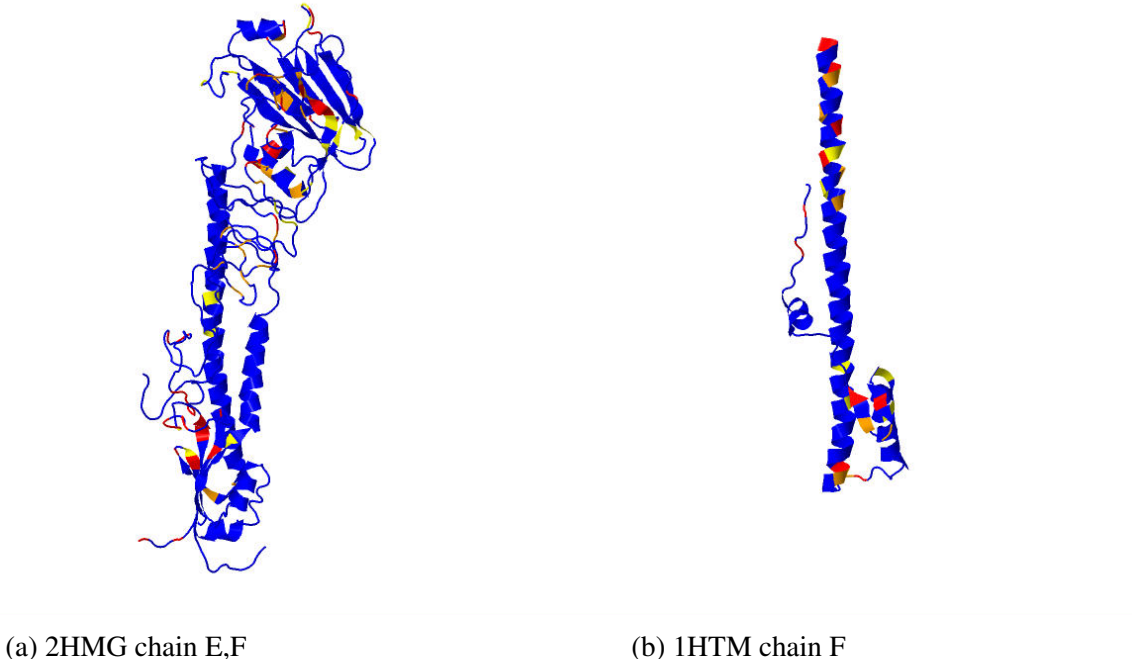
is taken as a descriptor of the point p in SO(3). By the quasi Boltzmann ansatz, differences  $\Pi(p_1) - \Pi(p_2)$  agree with free energy differences in  $kT_C$  units between protein features corresponding to  $p_1, p_2$ .

The histogram of  $\Pi(p)$  over HQ60 in  $kT_C$  units (henceforth the units  $kT_C$  in  $\Pi$ -values are usually suppressed) is given in SM Figure 5A. Taking a normalizing shift to the left of -2 kcal/mole= -2.9 $kT_C$  for the nominal free energy [14] of an  $\alpha$  helix as that of the ideal  $\alpha$  helix, which has  $\Pi = \ln 1 = 0$ , the free energy for the protein feature stabilized by p is given by  $[\Pi(p) - 2.9]kT_C$ . This scheme assigns absolute free energies to protein features and justifies computing these quantities separately for sub-units of an entire protein. The  $\Pi$ -values themselves will be employed in the sequel. A BHB with  $p \in SO(3)$  is exotic if  $\Pi(p) \geq 7.5$ , and a residue  $N_i - C_i^{\alpha} - C_i$  is exotic if either  $N_i$  or  $C_i$  participates in an exotic BHB. In fact,  $\Pi(p) \geq 7.5$ , 8.5, 9.5 and 9.85 essentially correspond to the respective 90th, 95th, 99th and 100th percentiles of  $\Pi$ -values across HQ60.

# **Results**

Representative concrete examples of glycoproteins treated in [9] are analyzed in detail here, namely, for the influenza, paramyxovirus, tick-borne encephalitis and vesicular stomatitis viruses. Influenza is taken as a case in point in order to explain these several analyses.

Required for complete investigation here are both pre- and postfusion 3d structures, as re-



Jmol

Figure 3: Conformations of influenza type 3 hemagglutinin HA (a) chains E,F prefusion and (b) chain F postfusion, where chain E is cleaved *in vivo* preceding fusion. Blue indicates unexotic residues, and yellow, orange and red respectively correspond to  $\Pi$ -value at least 7.5, 8.5 and 9.5, i.e., the respective 90th, 95th and 99th percentiles.

spectively provided for a fixed strain of influenza hemagglutinin HA by PDB files 2HMG and 1HTM. However, either conformation alone could provide relevant data for drug or vaccine design. Concentrating now on just one monomer of the trimer HA, the exotic BHBs for chains E and F prefusion and chain F postfusion are computed by the methods here and enumerated in Table 1 in order of non-decreasing Π-values; for chain F, the exotic residues lying in the fusion peptide are highlighted in boldface prefusion but are absent postfusion since the fusion peptide itself is missing from the PDB file. These results are depicted in Figure 3, which is to be compared with [9, Figures 6b,c] where the functions of various peptides in chain F are explained as next discussed.

For chain F prefusion: residues 4,5 form the fusion peptide with 9,10,11 and 14,15 the

nearby loop; 62,63 account for helix extension; 96,101 account for C-terminus inversion; 172,175 form the C-terminus linker; 21,24,36 account for movement of the fusion peptide; residues 126,130,134,136,137 are of function unmentioned in [9], which emphasizes fusion peptides, and reorganize postfusion to form the C-helix. For chain E prefusion, which is also not considered in [9], the residues 135,136,137 and 221,227 pinpoint the sialic acid binding site with the other exotic residues of unknown function.

Thus are all of the exotic residues in chain F prefusion explained by function in [9], and only these arise from the method. For the other three viruses from [9] which are treated in SM, the analogous narrative comparisons are also substantive.

In order to provide a quantitative measure of the predictive power of the methods here, define a residue of a viral glycoprotein to be *active* if one of its standard conformational angles  $\phi$  or  $\psi$  changes by at least 180 degrees from pre- to postfusion conformation. The basic quantifiable assertion is that a prefusion exotic residue is at most one residue away along the backbone from an active one (though the reverse implication does not hold).

To test this hypothesis, the residues common to the pre- and postfusion conformations must be aligned, and this is accomplished in SM Table 1 for HA chain F. One finds R=122 residues common to the two conformations and that there are b=33 active residues, and c=19 inactive residues that are next to an active one with a=70 that are not. A trial producing  $n_b, n_c, n_a$  of these respective types has the natural trinomial probability given by  $\binom{n_a+n_b+n_c}{n_a}\binom{70}{122}^{n_a}(\frac{33}{122})^{n_b}(\frac{19}{122})^{n_c}$ , and the triples  $(n_a, n_b, n_c)$  admit the natural lexicographic order derived from  $\leq$  on the first and  $\geq$  on the remaining two entries. See SM for further detail.

The 7 exotic prefusion residues displayed in SM Table 1 are numbered 62, 96, 101, 130, 134-136, with  $n_a = n_b = 3$  and  $n_c = 1$ , and one computes a p-value of  $6.2 \times 10^{-3}$ . The other three examples give likewise statistically quite meaningful results based upon 168 further exotic residues among 1329 total residues common to pre- and postfusion conformations for the four

glycoproteins, as presented in SM Table 2. SM Table 3 likewise presents *p*-values for the other examples discussed in detail in [9] based upon their exotic BHBs presented in SM Table 4.

SM Table 5 provides the exotic residues for a host of viral glycoproteins in analogy to Table 1 or SM Table 4. Another validation of the method here is that there is evidently fine agreement in SM Table 5 between the tables and the known fusion loops with a few exceptions as noted. Moreover in all cases scrutinized for receptor binding domain, the tables compare favorably with the literature. SM Table 6 presents exotic BHBs for a collection of non-enveloped viral capsids, about which much less is known, and provides the first explicit predictions for their penetration peptides.

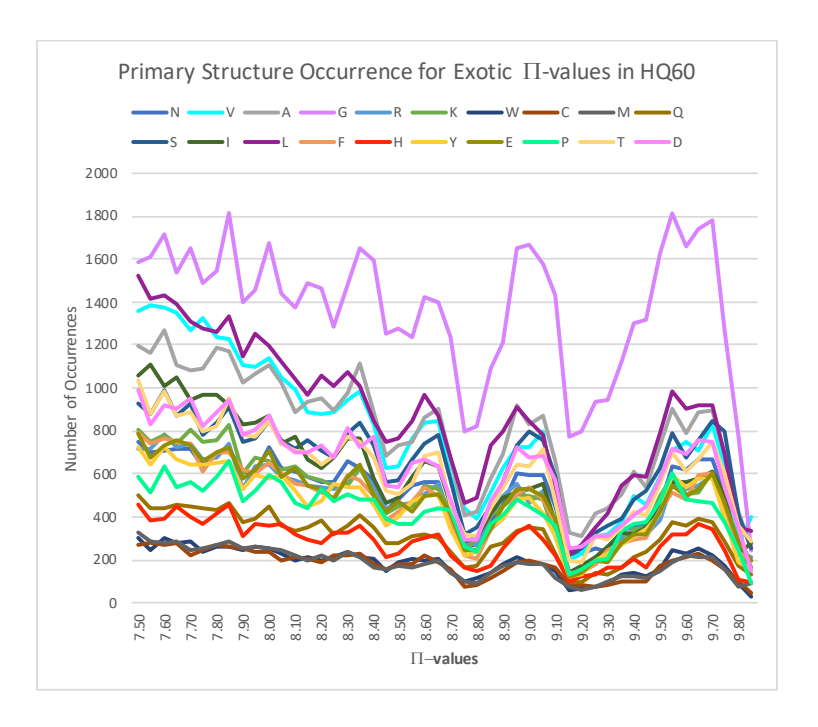


Figure 4: Histogram of  $\Pi$ -values and flanking primary structure for all exotic BHBs across HQ60. Curves are colored by residue as indicated. Notice the increasing frequency of glycine reflecting the presumably progressively contorted exotic features that the primary structure must support.

A striking phenomenon is evident in Figure 3: there are intervals of exotic free energy within which specific families of flanking amino acids vary together, one with another, where

the residues i, i+1, j-1, j are said to flank a BHB  $N_i - H_i :: O_j = C_j$ . This strongly suggests that there are characteristic primary structure motifs contributing to high free energy. These motifs should be retrievable with machine learning. More generally, this approach should open the possibility for backbone free energy estimation based upon primary structure alone, that is, a PDB file would no longer be necessary.

# **Discussion**

The overall point is that given the 3d prefusion structure of a viral glycoprotein, these methods furnish an ordered list of pairs of residues involved in exotic BHBs, and the latter entries among this list, those of highest free energy, provide most promising targets for antiviral drugs or vaccines. More refined predictions can be made by comparing exotic residues of viral glycoproteins pre- and postfusion, in complex with antibodies or in complex with receptors. Furthermore, there is the prospect with machine learning of making said predictions on the basis of primary structure alone.

There is the general pattern that fusion peptides and receptor binding domains are exotic, the latter typically less so than the former and the fusion loop hidden prefusion as for influenza and flaviviruses or only partially composed and exposed as for vesicular stomatitis or hidden as for tick-borne encephalitis. Based on this scant circumstantial evidence, one might ask whether the host immune system can detect exotic protein features.

It is worth emphasizing that this idea of estimating free energies using exotic protein features in order to locate conformationally active sites must surely be more widely applicable in protein science and structural biology, for example in tyrosine kinase receptors, for which there are promising preliminary results. Other seemingly natural candidates for the method include certain prion, transmembrane, signal transduction and cell motility proteins.

# References

- [1] N. J. Dimmock, A. J. Easton, K. N. Leppard (2007), *Introduction to Modern Virology* (Blackwell Publishing, 6th edition).
- [2] A. J. (1992) Viruses (Scientific American Library).
- [3] S. Shanker, S. Ramani, R. L. Atmar, M. K. Estes, B. V. Venkataram Prasad (2017), Structural features of glycan recognition among viral pathogens. *Current Opinions in Structural Biology* 44, 211-218.
- [4] S. Boulant, M. Stanifer, P.-Y. Lozach (2015), Dynamics of Virus-Receptor Interactions in Virus Binding, Signaling, and Endocytosis. *Viruses* **7**(6), 2794-2815.
- [5] M. G. Rossman (1994), Viral cell recognition and entry. *Protein Science* **3**(10), 1712-1725.
- [6] L. V. Chernomordik, M. M. Kozlov (2009), Mechanics of membrane fusion. *Nature Structural and Molecular Biology* **15**(7), 675-683.
- [7] S. C. Harrison (2008), Viral membrane fusion. *Nature Structural Molecular Biology* **15**(7), 690-698.
- [8] J. A. Thorley, J. A. Keating, J. Z. Rappoport (2010), Mechanisms of viral entry: sneaking in the front door. *Protoplasma* **244**, 15-24.
- [9] J. M. White, S. E. Delos, M. Brecher, K. Schomberg (2008), Structures and mechanisms of viral membrane fusion proteins: multiple variations on a common theme. Critical of reviews in Biochemistry and Molecular Biology 43, 189-219.

- [10] B. Tsai (2007), Penetration of nonenveloped viruses into the cytoplasm. *Annual Reviews Cellular and Developmental Biology* **23**, 23-43.
- [11] C. L. Moyer, G. R. Nemerow (2011), Viral weapons of membrane destruction: variable modes of membrane penetration by non-enveloped viruses. *Current Opinions in Virology* **1**(1), 44-49.
- [12] P. W. Choppin, A. Scheid (1980), The Role of Viral Glycoproteins in Adsorption, Penetration, and Pathogenicity of Viruses. *Reviews of Infectious Diseases* **2**(1), 40-61.
- [13] Viral Glycoprotein Structure, Viruses-Special Issue, editor A. Ward (2015).
- [14] A. V. Finkelstein, O. Ptitsyn (2016), *Protein Physics, A Course of Lectures* (Academic Press, 2nd edition).
- [15] F. M. Pohl (1971), Empirical protein energy maps. *Nature New Biology* **234**, 277-279.
- [16] A. V. Finkelstein, A. M. Gutin, A. Ya Badretdinov (1995), Boltzmann-like statistics of protein architectures: Origins and consequences. *Sub-cellular Biochemistry* **24**, 1-26.
- [17] Finkelstein, A. Ya Badretdinov, A. M. Gutin (1995), Why do protein architectures have Boltzmann-like statistics? *Proteins* **23**, 142-150.
- [18] H. M. Berman, J. Westbrook, Z. Feng, G. Gilland, T. N. Bhat, H. Weissig, I. N. Shindyalov, P. E. Bourne (2000), The Protein Data Bank. *Nucleic Acids Research* 28, 235-242.
- [19] R. C. Penner, E. S. Andersen, J. L. Ledet, A. K. Kantcheva, M. Bublitz, P. Nissen, A. M. H. Rasmussen, K. L. Svane, B. Hammer, R. Rezazadegan, N. C. Nielsen, J. T.

- Nielsen, J. E. Andersen (2014), Hydrogen bond rotations as a uniform structural tool for analyzing protein architecture. *Nature Communications* **5**, 5803.
- [20] G. Wang, R. L. Dunbrack, Jr. (2003), PISCES: a protein sequence culling server. *Bioinformatics* **19**,1589-1591.
- [21] W. Kabsch, C. Sander (1983), DSSP: definition of secondary structure of proteins given a set of 3D coordinates. *Biopolymers* **22**, 2577-2637.
- [22] T. Smith, M. S. Waterman (1981), Identification of Common Molecular Subsequences. *Journal of Molecular Biology* **147**(1), 195-197.
- [23] T. J. Tuthill, D. Bubeck, D. J. Rowlands, J. M. Hogle (2006), Characterization of Early Steps in the Poliovirus Infection Process: Receptor-Decorated Liposomes Induce Conversion of the Virus to Membrane-Anchored Entry-Intermediate Particles. *Journal of Virology* 80(1), 172-180.
- [24] Y. He, V. D. Bowman, S. Mueller, C. M. Bator, J. Bella, X. Peng, T. S. Baker, E. Wimmer, R. J. Kuhn, M. G. Rossman (2000), Interaction of the poliovirus receptor with poliovirus. *Proceedings of the National Academy of Sciences* 97(1), 79-84.
- [25] O. Carugo (2018), How large B-factors can be in protein crystal structures? *BMC Bioinformatics* **19**(61).

Acknowledgements: It is a pleasure to thank Minus van Baalen, Thibault Damour, Misha Gromov, Pablo Guardado-Calvo, Nadya Morozova, Sergiy Garbuzynskiy and Mike Waterman for valuable comments and inspiration. But the deepest thanks are to Alexeii Finkelstein for his guidance, patience and critical readings of earlier versions of this manuscript. Thanks are furthermore due to Karim Ben Abdallah, Jakob Trousdal Nielsen and especially Ebbe Sloth Andersen and Greg McShane for computer assistance. The author has no competing interests.

# Table 1: Exotic Residues for Influenza HA

# Influenza Virus Type A Glycoprotein HA Prefusion (2HMG)

### Chain E

90-94% 116/111 241/170 258/121 16/F136 256/150 86/57 158/160 221/227

95-98% 284/286 288/50 150/72 253/181 65/61 308/293 114/109 304/F62 135/153 157/194 137/146 142/144

99% F15/17 161/157 F24/16 74/68

100% 19/F21 20/F14 29/31 95/63 106/102 124/255 147/136 198/195 207/209 254/152 F63/303

### Chain F

90-94% E16/136 36/24 101/96 9/5

95-98% 130/126

99% 15/E17 24/E16

100% E19/21 E20/14 10/4 11/5 63/E303 134/137 175/172

# Influenza Virus Type A Glycoprotein HA Postfusion (1HTM)

### Chain I

90-94% 128/123 61/56 92/87

95-98% 63/59 107/103 134/137 50/45

99% 132/139

100% 44/40 57/52 108/102 160/157

Donor/Acceptor residues of exotic BHBs in order of non-decreasing  $\Pi$ -values with 7.5, 8.5, 9.5 and 9.85 respectively corresponding to percentiles 90, 95, 99 and 100. Residues lying in the fusion peptide are highlighted in boldface.

**List of Supplementary Materials:** Methods; Mathematical methods; Narrative discussion of test cases; Non-enveloped viral capsids; Computation of *p*-values; Energetics of Flanking Structures; SM Figures 1-4; SM Tables 1-6.

# Supplementary Material

### 1. Methods

A Dictionary of Secondary Structure for Proteins (DSSP) [21] prospective BHB N-H :: O = C is accepted provided that furthermore |H-O| < 2.7Å, |N-O| < 3.5Å and  $\angle$  NHO,  $\angle$  COH > 90°.

Using lower quality 3d structures and both higher and lower homology identity establish robustness of the basic properties of the distribution of BHBs from HQ60 in SO(3) over the data employed to compute it. Moreover, one must confirm that these constraints are not simply steric in nature, and indeed in excess of 95% of SO(3) is achievable by pairs of peptide groups at the distance scale of hydrogen bonds. On the other hand, the constraints are partly quantum physical insofar as a Density Functional Theory solution of the Schrödinger equation [19] for pairs of peptide groups essentially recovers the empirically discovered region. In fact, within this subspace containing all BHBs in HQ60, there is evident grouping into 30 distinct regions, various attributes of which are given [19, Table 1]. However, this clustering is entirely immaterial to the considerations of the current manuscript. Indeed, a recent further analysis within clusters (which is not presented here) reveals that they are highly anisotropic and fail to remotely resemble a normal distribution therein, thus the attention here only on the PDB-derived distribution depicted in Figure 2. Given two peptide groups, there is not only the rotation between them, but also the displacement between their N-terminal alpha carbons, and one might wonder about including these translations as a further aspect of peptide group comparison; it was determined already in [19] that this adds nothing since the translation is essentially determined by the rotation.

The server https://bion-server.au.dk/hbonds/ for a given PDB file returns a list of its BHBs together with the density d(p) relative to HQ60 of each BHB as discussed in the main text. The BHBs are then rank-ordered by  $\Pi$ -values, and only those exceeding the percentile cutoffs are considered.

Extensive tables of viral glycoproteins are presented in SM Tables 5 and 6. Indicated in boldface are the residues lying in generally agreed upon fusion loops, which are taken  $\pm 2$  residues to reflect uncertainty in precise peptide boundaries. Several table entries are *not* fusion peptides but are included in the table to illuminate for instance receptor binding domains.

A few words are in order about the method in general and these tables in particular: Comparison with the residue B-values reported in the PDB files should be taken into account with large B-values (which measure the disorder of the protein, cf. [25]) at a residue presumably casting potential doubt upon the verity of the reported high free energy. At the same time, the exotic residues determined here for PDB files with large reported resolutions might likewise be questioned though an extensive study of influenza virus type A hemagglutinin (not reported here) found the resulting exotic residues basically insensitive to reasonable resolutions, say, less than about 3.5-4.0 Angstrom.

1

### 2. Mathematical Methods

Several data are not indicated in Figure 1: the distance |i-j| of residues along the backbone, the length  $|O_j - H_{i+1}|$  of the BHB and the backbone conformational angles  $\psi_i$  and  $\phi_{i+1}$ , the respective rotation angles about the  $C_i^{\alpha}$ - $C_i$  and  $N_{i+1}$ - $C_{i+1}^{\alpha}$  axes.

Here is another explanation of the descriptor in SO(3) associated to a BHB in Figure 1: The cross product (in this order) of displacement vectors  $\overrightarrow{C_i^{\alpha}C_i}$  and  $\overrightarrow{C_iO_i}$  determines a unit vector perpendicular to the plane of peptide group  $\overrightarrow{P_i}$ , and this plane contains the unit vector parallel to the displacement vector  $\overrightarrow{C_iN_{i+1}}$  of the peptide bond. The cross product of these (in this order) determines a third vector. There is a unique 3d rotation  $A_{P_i}$  mapping unit vectors parallel to the z-, x-, and y-axes, respectively, to these three vectors (in these orders), and likewise  $A_{P_j}$  for the peptide group  $P_j$ . In order to obtain a result which is independent of the position of the pair  $P_i$ ,  $P_j$  in space, one applies to the entire configuration the rotation  $A_{P_i}^{-1}$  as illustrated on the right of Figure 1 and achieves the result  $A_{P_i}^{-1}A_{P_j}$  as the rotation in SO(3) associated to the pair  $P_i$ ,  $P_j$ .

Figure 2 illustrates the histogram of BHBs in HQ60, where the space SO(3) of 3d rotations is depicted as a ball. To explain this, start by observing that a 3d rotation is determined by an axis L of rotation and an angle  $-\pi \le \theta \le \pi$  of rotation about it, a fact that goes back to Gauss. If the unit vector  $\vec{u}$  is parallel to L, then the interval of all multiples  $\theta \vec{u}$  therefore corresponds to all rotations with axis L including the trivial rotation corresponding to  $\theta = 0$ , where  $\pi \vec{u}$  and  $-\pi \vec{u}$  evidently describe the same 3d rotation, namely by  $\pi$  or by  $-\pi$  about L.

The collection SO(3) of all 3d rotations can therefore be visualized as a 3d ball of radius  $\pi$  with each pair  $\pm \pi \vec{u}$  of points in its boundary 2d sphere identified to a separate single point. The particular representation in Figure 2 of the distribution in SO(3) was chosen to minimize the density proximal to the boundary. The *ideal* (right-handed) alpha helix has its conformational angles  $\phi = -65^{\circ}$  and  $\psi = -40^{\circ}$  and here has its 3d rotation described by  $\theta = 1.086$ ,  $\vec{u} = (-0.315, 0.935, -0.164)$ . This element of SO(3) occurs at the point of highest density in HQ60, as is evident in the middle of the fourth row from the top in Figure 2. Other local maxima for the density which are clear in the figure are studied in the cluster analysis of [19].

# 3. NARRATIVE DISCUSSION OF TEST CASES

For the test cases, essentially all of the prefusion exotic residues in SM Table 4 accord perfectly with expectations from [9] as next detailed. SM Figure 1 depicts the various glycoproteins aligned to Figure 6 of [9] to which it should be compared. The color scheme here is that blue indicates non-exotic, yellow above the 7.5 cutoff, orange above the 8.5 cutoff and red above the 9.5 cutoff for  $\Pi$ -values, which respectively correspond to the 90th, 95th, and 99th percentiles. As a notational convenience for this discussion, if the residue N is involved in an exotic BHB, then one writes Nb, Ny, No, Nr to indicate this discretization of  $\Pi$ -values into colors also letting Nx indicate that N is involved in an exotic BHB with the 100th percentile  $\Pi$ -value of 9.85.

Influenza (PDB files 2HMG, 1HTM): See Figure 1A-D and 2A-B. As per [9] for chain F prefusion: residues 4x,5x form the fusion peptide with 9y,10x,11x and

14x,15r the nearby loop; 62o,63x account for helix extension; 96y,101y account for C-terminus inversion; 172x,175x form the C-terminus linker; 21x,24r,36y account for movement of the fusion peptide; 126o,130o,134x,136x,137x are of function unmentioned in [9] prefusion and reorganize postfusion to form the C-helix. For chain E prefusion, the residues 135o,136x,137o and 221y,227y pinpoint the sialic acid binding sites with the others of unknown function. Illustrated in Figure 2A-B is the full hemagglutinin glycoprotein including the sialic acid receptor binding domain, which is also comprised of exotic BHBs.

Paramyxovirus (PDB files 2B9B, 1ZTM): See Figures 1E-H and 2C-D. There is only approximate consensus among the three chains A,B,C. For the prefusion chain A,B,C consensus exotic residues as per [9] and using the color scheme of Chain C depicted in Figure 3: 90x,91x,92,93,94r,95o,96x lie in the fusion peptide; 264x,269r lie at the C-terminus of the helix extension domain; 2970,2990 lie adjacent to the C-terminal inversion domain; 484y lies in the C-helix; 330r lies in a loop in Domain II; 4140,416y lie in a loop in Domain I. Concentrating just on Chain C and considering only colors R,X: 43x lies at the beginning of a  $\beta$  strand in DIII prefusion and in the middle of a  $\beta$  sheet postfusion; 90x,91r,94r,96x,102x,109x,113xlie in the fusion peptide, 184x,188x,189x lie in the C-terminus extension domain; 263r,264r,268x,269x lie in a loop and  $\beta$  turn region prefusion and comprise a  $\beta$ sheet postfusion; 278x lies in a loop between DI and DII prefusion and comprise a  $\beta$  sheet postfusion; 328r,330r lie in a  $\beta$  turn region prefusion and in a short  $\beta$ sheet postfusion; 387x,388x,392x,393x,408x,424x lie in a short  $\beta$  sheet prefusion and comprise a loop postfusion; 469r,473r,480x,485x lie in the C-terminus inversion domain. All R,X bonds of Chain C prefusion exhibit postfusion DSSP secondary structure reconformation consistent with expectations.

Tick-borne Encephalitis (PDB files 1SVB, 1URZ): See Figure 1I-K. Concentrating here primarily on O,R prefusion as per [9]: 307y,3090 lie in the inversion loop; the fusion peptide is not exotic prefusion although residues 74,78,100,101,105,106 all have  $\Pi$ -values above 7.0, significant but below the cutoff, however with colors 74y,78y,100x,106x postfusion; the ij loop is unremarkable prefusion, but postfusion contains 248x,249x,251x,252x; 1480 prefusion lies in a loop in DI that is not exotic postfusion; in contrast, 1670,1690 prefusion also lie in a loop in DI which however becomes red postfusion; 1840 lies in the middle of a  $\beta$  strand both pre- and postfusion; 2780,2800 lie in a loop prefusion and in a  $\beta$  turn postfusion; 360r,366r,368r lie in a loop in DII prefusion that remains red postfusion; 3720,373r lie in the middle of a  $\beta$  strand in DI both pre- and postfusion but colored 372b,373y postfusion; 3880,3940 lie at the beginning and end, respectively, of a  $\beta$  strand prefusion and likewise postfusion but with an orange residue now between them. It appears that the fusion peptide is not composed of exotic residues until after the pre- to postfusion transition and that the ij loop is unremarkable pre- and exotic postfusion. Moreover, all of 1480,3720,373r appear to lose free energy in the pre- to postfusion transition. In contrast 1670,1690 and 360r,366r,368r become or remain red postfusion suggesting either possible false positives or some further activity involving them to follow the postfusion conformation. Meanwhile 2780,2800 undergo transition from loop to  $\beta$  turn consistent with losing free energy for reconformation; in contrast 3880,3940 retain their  $\beta$  strand conformation but decrease free energy and produce an orange residue between them postfusion.

Vesicular Stomatitis (PDB files 5I2S, 5I2M): See Figure 1L-O. As per [9] prefusion: extension domain 1 has no BHBs at all except for the nearby exotic 183y,185y, while extension domain 2 contains the exotic 29r,33r,38o; the fusion peptide is not exotic prefusion and contains 115y,118o,119y and 71o,72y,75y postfusion. Considering only O,R,X there are two general rules from pre- to postfusion transition: DSSP secondary structure conformation is preserved; and the free energy is non-increasing. The notable exceptions are: the loop 261x changes conformation to the end of a short  $\beta$  261o; the loop 404x at the C-terminus becomes the short  $\beta$  404o; the end of the  $\beta$  strand plus loop 370r,373r becomes the more exotic 370x,373x; the loop 10x becomes 12r,15r. Except for these few cases and the fusion peptide, the free energy of exotic peptides is again diminished or preserved from pre- to post-fusion, and all residues which are exotic postfusion are already exotic in the prefusion conformation. This finding is consistent with the fact that this glycoprotein is capable of oscillating between its pre- and postfuson conformations.

### 4. Non-enveloped Viral Capsids

SM Table 6 displays exotic residues for a selection of non-enveloped viral capsids, about whose recognition/binding and penetration mechanisms much less is known [10, 11]. For the best studied polio virus, the exotic regions of VP1 adjacent to VP4 interior to the capsid are consistent with what is in the literature [23, 5], where VP1 and VP4 are implicated in penetration, although VP4 itself contains only one exotic residue. Moreover, appropriate residues in the canyon walls presumed to be associated with receptor binding [24, 5] are found to be exotic for both polio and rhinovirus. By analogy for the other entries in SM Table 6 under the assumption that penetration peptides must be shielded from the immune system, the exotic residues interior to the capsids provide natural predictions for penetration peptides as do the exotic exterior residues for receptor binding domains.

# 5. Computation of p-values

SM Table 2 provides a summary of the conformational activity of exotic residues in analogy to the discussion in the main text derived from SM Table 1 for influenza HA, but the aligned pre- and postfusion DSSP data akin to SM Table 1 for paramyxovirus, tick-borne encephalitis and vesicular stomatitis are not presented here, only their summary in SM Table 2. In fact, for paramyxovirus, there are available only two different strains for pre- and postfusion conformations which are aligned using the Smith-Waterman algorithm [26].

SM Table 3 presents the p-values based upon data in SM Table 2. For each of the four examples let R denote the total number of residues common to pre- and post-fusion conformations and  $n_a$ ,  $n_b$  and  $n_c$  denote the respective number of residues further than one away from an active residue, the number of active residues and the number of inactive residues next to an active one along the backbone. The natural trinomial probability density is

$$P(n_a, n_b, n_c) = \binom{n_a + n_b + n_c}{n_a \ n_b \ n_c} (\frac{a}{R})^{n_a} (\frac{b}{R})^{n_b} (\frac{c}{R})^{n_c}.$$

These data R, a, b, c are reported in the first four columns of SM Table 2 and then used in this way to compute probabilities for the trials given in SM Table 3.

The computation of p-values furthermore requires a linear ordering for tails, which is also naturally given where  $(n_a, n_b, n_c) \leq (n'_a, n'_b, n'_c)$  provided  $n_a \leq n'_a$  with equality only if  $n_b \geq n'_b$  with equality only if  $n_c \geq n'_c$ , or in other words, lexicographic ordering on triples  $(n_a, n_b, n_c)$  derived from  $\leq$  on the first and  $\geq$  on the remaining two entries.

Call an exotic prefusion residue dissipative if its free energy is not exotic postfusion and call it conservative otherwise, where each determination is made within one residue of the prefusion exotic residue. It is arguably only the dissipative case that provides possible false positives in SM Table 3 since a conservative residue has not expended free energy presumably preserved for later conformational activity. This distinction is especially pertinent for vesicular stomatitis virus glycoprotein G which is exceptional since it can oscillate back and forth between pre- and postfusion conformations.

The statistical significance for influenza and tick-borne encephalitis reported for the first p-values in SM Table 3 is compelling as it stands. The comparatively less significant but still acceptable first p-value for paramyxovirus likely reflects that different strains are aligned pre- and postfusion. The second p-value is tailored specifically for vesicular stomatitis to account for its conserved exotic residues evidently preserving free energy.

### 6. Energetics of Flanking Structures

The residues i, i+1, j-1, j are said to flank a BHB  $N_i - H_i :: O_j = C_j$ . Figure 4 of the main text plots flanking primary structure type across the exotic range of free energies and illustrates that there are characteristic peptides of high free energies which might be discovered with machine learning.

SM Figure 3 illustrates the analogous distribution of primary structure across the entire free energy spectrum. Owing to their different magnitudes, the collection of residues is partitioned into three comparable sets as indicated for ready comparisons. As in the exotic tail in Figure 4 of the main text, again there appear to be characteristic peptides not as there of high but here of low and other free energies which might be discovered through machine learning.

The histogram of  $\Pi$ -values for BHBs over all of HQ60 is given in Figure 4A, and the distribution of DSSP flanking secondary structure types for HQ60 across the free energy spectrum is shown in Figure 4B. Note the predominance of  $\alpha$  helices for small and the mixture of all types for large free energy.

It gives an internal consistency check that the overall shift to the left of the histogram in Figure 4A by -2 kcal/mole as explained in the main text gives a maximum free energy just below the bounds of protein stability.

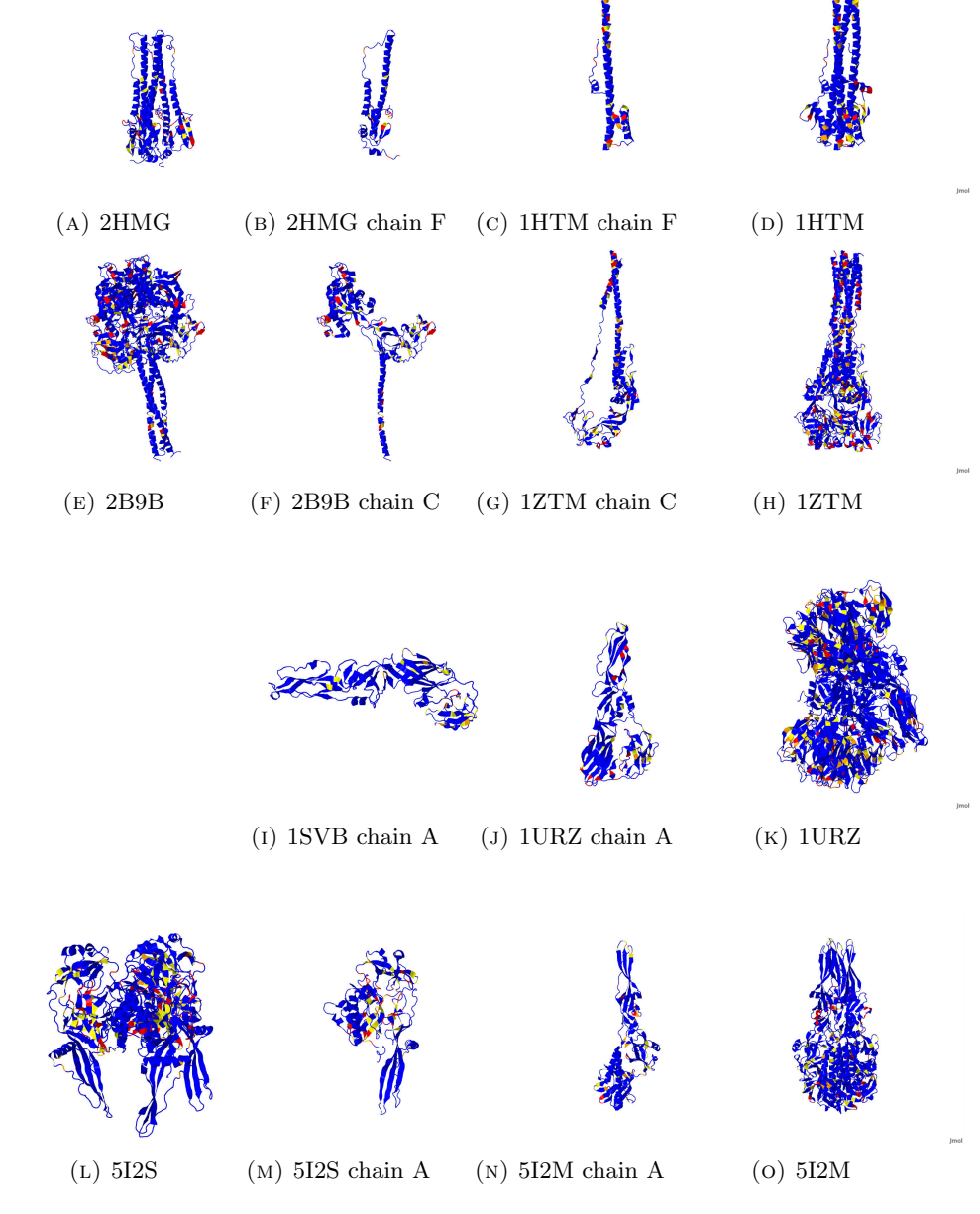


FIGURE 1. Compare with Figure 6 in [9], to which these images are aligned. Blue indicates non-exotic, and yellow, orange and red respectively correspond to Π-value at least 7.5, 8.5 and 9.5. Parts A,B are influenza hemagglutinin pre- and parts C,D postfusion. Parts E,F are paramyxovirus glycoprotein F pre- and parts G,H postfusion. Part I is tick-borne encephalitis glycoprotein E pre- and parts J,K postfusion. Parts L,M are vesicular stomatitis glycoprotein G pre- and parts N,O postfusion.

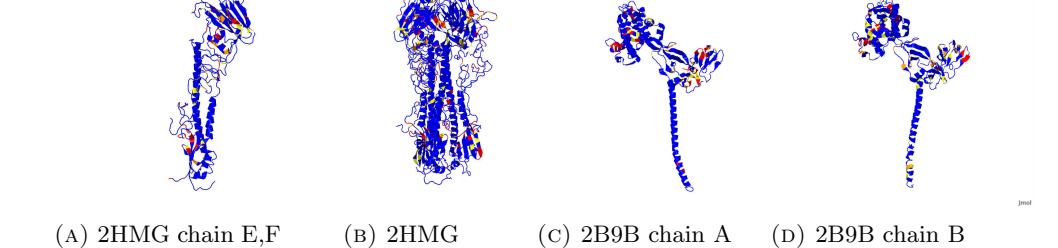


FIGURE 2. Blue indicates non-exotic, and yellow, orange and red respectively correspond to  $\Pi$ -value at least 7.5, 8.5 and 9.5. Part A illustrates exotic regions for influenza hemagglutinin HA1 and HA2 chains E and F, and B illustrates the entire glycoprotein. Parts C and D respectively depict 2B9B chains A and B for comparison with 2B9B chain C, which is illustrated in part F of SM Figure 1.

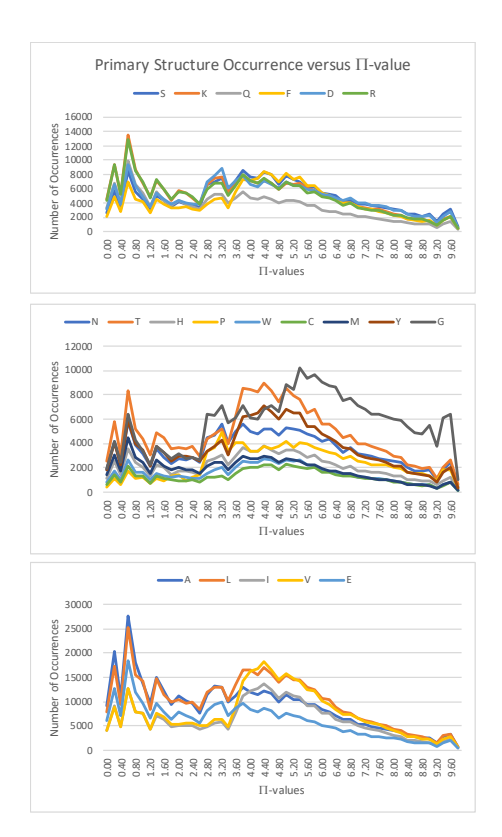
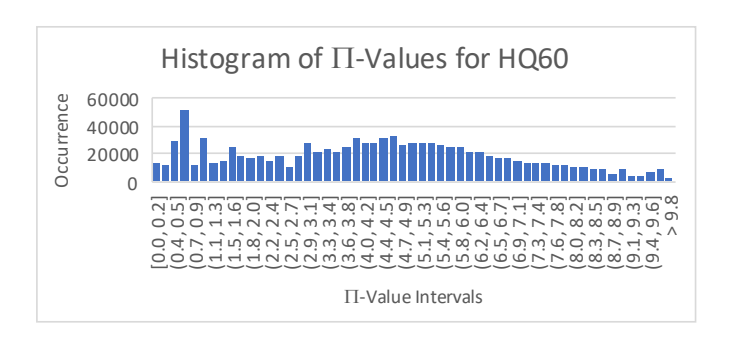
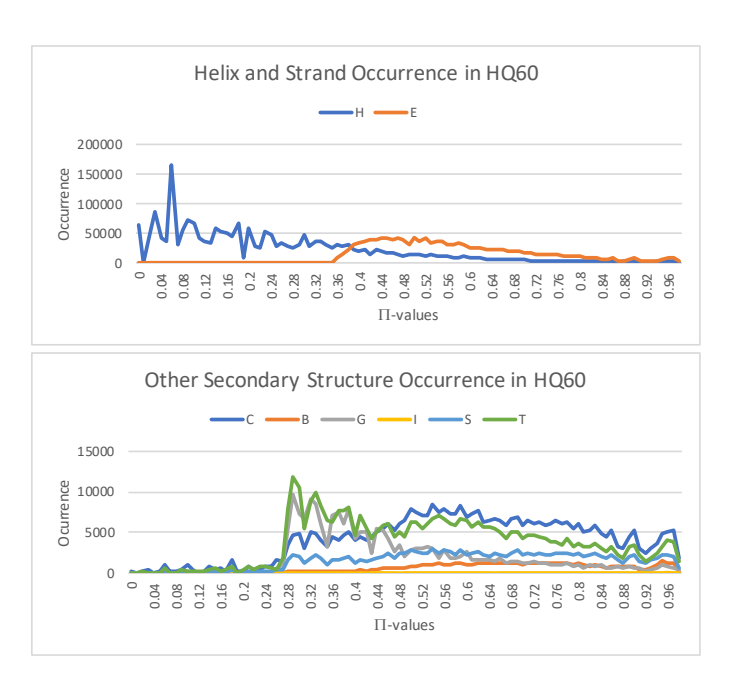


FIGURE 3. Histogram of  $\Pi$ -values and flanking primary structure for all BHBs across HQ60. Compare to SM Figure 3.



(A) Histogram of  $\Pi(p) = \ln(d(m)/d(p))$  for all BHBs across HQ60. The x-axis corresponds to the indicated intervals of  $\Pi$ -values achieved for the BHBs in HQ60, and the y-axis indicates the number of occurrences in HQ60 within each interval of size 0.18.



(B) Population of flanking DSSP secondary structure types H ( $\alpha$  helix), E ( $\beta$  strand), C (coil), B ( $\beta$  bridge), G (3<sub>10</sub> helix), I ( $\pi$  helix), S (bend), and T (turn) across the range of  $\Pi$ -values along the x-axis.

FIGURE 4. Histogram of  $\Pi$ -values and of flanking DSSP secondary structure types across HQ60.

Table 1. Aligned Pre/Postfusion Influenza HA chain F

Residue	$\phi_{ m pre}$	$\psi_{\mathrm{pre}}$	$\phi_{ m post}$	$\psi_{ m post}$	$\Delta \phi$	$\Delta \psi$	$\Pi_{\mathrm{pre}}$	$\Pi_{\mathrm{post}}$
40	-69	-34.4	-69	-71.6	0	37.2	0.85	9.85
41	-60.2	-42.2	-39.4	-53.7	20.8	11.5	4.18	0.7
42	-68	-43.9	-59	-38	9	5.9	2.73	2.15
43	-53.7	-47.9	-74.6	-32.2	20.9	15.7	3.34	3.26
44	-63.2	-49.3	-60.9	-53.9	2.3	4.6	1.46	9.85
45	-62.4	-44	-61.8	-29.4	0.6	14.6	0.85	9.02
46	-59.3	-48	-73.6	-31.4	14.3	16.6	4.18	1.56
47	-57.1	-44.1	-71.3	-46.1	14.2	2	2.73	3.41
48	-66.5	-36.9	-54	-58.3	12.5	21.4	3.34	4.77
49	-68.5	-34	-63	-30.9	5.5	3.1	4.06	3.63
50	-62.3	-50.5	-76.5	-22.1	14.2	28.4	0.68	9.02
51	-67.3	-37.6	-82.7	-43.3	15.4	5.7	2.43	2.73
52	-59	-42.2	-59	-37.3	0	4.9	1.28	9.85
53	-69.7	-36.6	-78.8	-18.6	9.1	18	2.3	3.09
54	-64.5	-35.3	-71.1	-37.7	6.6	2.4	6.87	4.83
55	-70.6	-38.4	-69.3	-66	1.3	27.6	0.39	5.1
56	-86.1	10.8	-44.7	-44.3	41.4	55.1	1.56	8.35
57	-62.5	-163.4	-61.9	-49.6	0.6	113.8	0.39	9.85
58	-57.1	125.2	-66.6	-40	9.5	165.2	6.87	3.09
59	-74.1	135.8	-61	-60.1	13.1	164.1	0	8.7
60	-83.1	140.5	-40.7	-42	42.4	177.5	0	5.1
61	107.8	141.2	-72.9	-38.6	179.3	179.8	0	8.35
62	130.9	146.5	-64.2	-49.8	164.9	163.7	9.85	4.55
63	112.8	-109.2	-50.8	-34.1	163.6	75.1	0	8.7
64	-67.7	123.7	-74.1	-36.1	6.4	159.8	0	4.93
65	125.5	-140.4	-74.2	-25	160.3	115.4	0	2.35
66	102.4	162.3	-69.7	-47.9	172.1	149.8	0	2.12
67	-72	149.9	-58.5	-39.4	13.5	170.7	0	5.35
68	129.1	8.7	-63.2	-45.2	167.7	53.9	0	2.35
69	144	135.6	-65.9	-38.4	150.1	174	0	1.03
70	128.8	146.2	-58.1	-38	173.1	175.8	0	6.22
71	118.3	15.8	-72.3	-39	169.4	54.8	0	3.47
72	141.9	155.8	-58.6	-44.5	159.5	159.7	0	2.66
73	-98.8	122.3	-63.6	-60.4	35.2	177.3	0	5.48
74	119.9	-24.6	-57.7	-23.4	177.6	1.2	0	4.64
75	94.7	-135	-76.8	-45.1	171.5	89.9	6.48	6.22
76	-52.6	-53.3	-65.8	-27.4	13.2	25.9	0.44	3.47
77	-67.3	-36.6	-69.9	-34.3	2.6	2.3	0.6	1.88
78	-71	-35.3	-75.6	-36.7	4.6	1.4	1.55	5.48
79	-58.6	-40.8	-60.4	-37.7	1.8	3.1	0.39	4.64
80	-69.6	-37.3	-68.7	-43.6	0.9	6.3	6.48	3.47
81	-63.1	-43.1	-58	-44.5	5.1	1.4	2.37	1.55
82	-67.6	-39.4	-64.7	-44.4	2.9	5	2.4	2.8
83	-65.4	-45.4	-69.2	-24.3	3.8	21.1	1.55	3.34
84	-55	-43.4	-71.6	-50.5	16.6	7.1	0.68	2.43
85	-76.9	-35.4	-52.6	-52.6	24.3	17.2	2.45	6.03
86	-70	-36	-62.5	-45.5	7.5	9.5	3.68	3.39
87	-75.2	-26.3	-55.6	-39.5	19.6	13.2	2.4	8.35
88	-63.4	-46.8	-67	-63.9	3.6	17.1	1.15	5.53
89	-62.5	-49.7	-50.1	-32.4	12.4	17.3	3.27	4.05
90	-61.6	-33.5	-64.9	-54.1	3.3	20.6	1.28	6.03
91	-68.3	-43	-61.3	-36.1	7	6.9	3.68	3.39
92	-70.3	-29.1	-71	-40.5	0.7	11.4	3.34	8.35
93	-71.9	-36.1	-66.8	-37.4	5.1	1.3	0.87	5.53
94	-61.9	-48.4	-57.1	-39.7	4.8	8.7	3.27	4.05
95	-56.4	-51.5	-56.1	-55	0.3	3.5	1.59	4.77
DSSP files	for OH	MC and	THTM.	1:		Alania -		rociduos

DSSP files for 2HMG and 1HTM are aligned along their common residues, conformational angles  $\phi_{\rm pre}$ ,  $\psi_{\rm pre}$  prefusion and  $\phi_{\rm post}$ ,  $\psi_{\rm post}$  postfusion are given, and differences  $\Delta\phi$  and  $\Delta\psi$  are computed. The maximum of the  $\Pi$ -values of the two prospective BHBs are reported  $\Pi_{\rm pre}$  pre- and  $\Pi_{\rm post}$  postfusion.

TABLE 1. (continued) Aligned Pre/Postfusion Influenza HA chain F

Residue	4	$\psi_{ m pre}$	Δ.	$\psi_{ m post}$	$\Delta \phi$	$\Delta \psi$	$\Pi_{\mathrm{pre}}$	$\Pi_{\mathrm{post}}$
Tesique	$\phi_{\mathrm{pre}}$	$\varphi_{\mathrm{pre}}$	$\phi_{ m post}$	$\varphi_{\mathrm{post}}$	Δφ	$\Delta \varphi$	11pre	11post
O.C	C1 0	94.4	CO 9	20.0	1.1	2.0	7.05	4.00
96 07	-61.9	-34.4	-60.8	-30.8	$\frac{1.1}{7.2}$	3.6	7.95	4.92
97	-71.8	-40.1	-79	-28.9	7.2	11.2	3.34	4.12
98	-72.4	-35.8	-75.1	-31.1	2.7	4.7	1.89	4.68
99	-59.9	-59.1	-58.8	-48.8	1.1	10.3	5.2	5.58
100	-62.7	-32.4	-64.6	-45.9	1.9	13.5	3.17	2.43
101	-61.2	-51.5	-68.2	-21.1	7	30.4	7.95	4.92
102	-62.3	-53.2	-81.2	-46.8	18.9	6.4	2.31	9.85
103	-47.4	-50.5	-52.6	-49.2	5.2	1.3	1.89	8.74
104	-66.6	-38.1	-59.3	-36.9	7.3	1.2	5.2	1.64
105	-63.7	-44.1	-80.2	3.8	16.5	47.9	3.17	2.21
106	-69.8	-37.5	67.6	10.3	137.4	47.8	1.47	3.29
107	-61.1	-42.5	-67.4	-11.3	6.3	31.2	2.04	8.74
108	-65.5	-36.3	-159.3	176.1	93.8	147.6	0.66	9.85
109	-77	-33.8	-144.2	111.8	67.2	145.6	2.01	4.23
110	-60.7	-48.8	-66.7	11.5	6	60.3	2.21	0
111	-68.6	-32.1	-94.2	-30.4	25.6	1.7	2.33	0
112	-61.4	-44.4	-54.9	118.5	6.5	162.9	3.76	6.86
113	-56.1	-54.3	-40.2	-45.6	15.9	8.7	3.6	4.23
114	-58	-39.5	-63.4	-45.8	5.4	6.3	2.01	6.89
115	-59.7	-52.4	-74.5	-37.4	14.8	15	3.29	2.8
116	-61.9	-34.7	-62.1	-29.6	0.2	5.1	2.33	6.86
117	-66.7	-42.2	-66.9	-49.9	0.2	7.7	3.76	7.08
118	-58.9	-43.9	-48.4	-51.9	10.5	8	3.6	3.95
119	-57.2	-51.1	-59.6	-45.5	2.4	5.6	2.01	6.89
120	-63.9	-36.2	-67.8	-10.9	3.9	25.3	3.29	2.8
121	-67.2	-44.2	-75.4	-57.8	8.2	13.6	0.94	3.18
122	-64.4	-41.4	-60	-41.1	4.4	0.3	0.68	6.25
123	-58.2	-47.2	-56.5	-30.8	1.7	16.4	1.56	7.79
124	-63.9	-34.2	-81.6	-21.7	17.7	12.5	4.46	3.87
125	-67.9	-40.9	-76.5	-45.5	8.6	4.6	0.85	6.96
126	-73.4	-9.1	-67.4	-57.7	6	48.6	9	3.98
127	40.7	-124	-47.6	-22.5	88.3	101.5	0.65	0.68
128	-88.8	14.3	-88.4	-60.6	0.4	74.9	4.46	7.79
129	-99.4	-3.7	-92	36.2	7.4	39.9	0	0
130	141.3	163.8	-172.7	160	46	3.8	9	6.96
131	130.4	147.8	-79.4	107.2	150.2	40.6	0	5.29
132	-75.1	131	-77.9	114.6	2.8	16.4	5.23	9.52
133	-94.5	4.7	-63.9	-40.7	30.6	45.4	0	0
134	74.8	7.6	124.6	-32.2	49.8	39.8	9.85	8.92
135	128.1	27.5	-100.1	21	131.8	6.5	7.83	0
136	86.2	-2.9	88.2	16.4	2	19.3	9.85	6.02
137	106.2	132.6	-111	145.6	142.8	13	0	8.92
138	-91.4	140.9	-131	136.5	39.6	4.4	0	4.02
139	-93.3	113.2	-96.8	109	3.5	4.2	5.23	9.52
140	-84.8	120.9	-95.1	112.2	10.3	8.7	5.68	5.66
141	-90.5	51.5	-88.5	142.6	2	91.1	0	4.93
142	170.6	164.3	-115.8	192.0 $101.7$	73.6	62.6	5.68	0
142	-69.9	119.8	-64.7	-25.4	5.2	145.2	0	0
143	127.8	91.4	-04.7	106.5	119	145.2 $15.1$	0	0
144	-67.1	176.8	-113.2 -74.1	178.9	7	$\frac{15.1}{2.1}$	7.29	$\frac{0}{2.74}$
$145 \\ 146$	-61.7	-24.1	-74.1 -63.1		1.4	$\frac{2.1}{5.4}$	$\frac{7.29}{2.51}$	$\frac{2.74}{4.73}$
				-29.5		$\frac{5.4}{26.1}$		
147	-79	-32.7	-68.8	-58.8	10.2		3.02	3.16
148	-64 -58.8	-46.9	-50	-51.1	14	4.2	2.73	4.41
149		-42.1	-56	-29.4	2.8	12.7	4.65	0 7.01
150	-65.6	-32.3	-69	-44.5	3.4	12.2	2.64	7.01

DSSP files for 2HMG and 1HTM are aligned along their common residues, conformational angles  $\phi_{\rm pre}$ ,  $\psi_{\rm pre}$  prefusion and  $\phi_{\rm post}$ ,  $\psi_{\rm post}$  postfusion are given, and differences  $\Delta\phi$  and  $\Delta\psi$  are computed. The maximum of the  $\Pi$ -values of the two prospective BHBs are reported  $\Pi_{\rm pre}$  pre- and  $\Pi_{\rm post}$  postfusion.

TABLE 1. (continued) Aligned Pre/Postfusion Influenza HA chain F

Residue	$\phi_{\mathrm{pre}}$	$\psi_{\mathrm{pre}}$	$\phi_{\mathrm{post}}$	$\psi_{\mathrm{post}}$	$\Delta \phi$	$\Delta \psi$	$\Pi_{\mathrm{pre}}$	$\Pi_{\mathrm{post}}$
151	-70.6	-28.5	-53.2	-41.7	17.4	13.2	6.14	6.4
152	-66.8	-44.7	-58.7	-12.2	8.1	32.5	3.02	4.41
153	-68.8	-35.9	-109.8	-49	41	13.1	2.73	4.06
154	-97.9	18.2	-45.4	-49.9	52.5	68.1	3.08	7.01
155	71.8	21	64.5	33.3	7.3	12.3	1.49	3.99
156	114.6	18.6	-95.8	136.6	149.6	118	4.62	6.4
157	-69.1	124.1	-153.6	106.6	84.5	17.5	6.14	9.85
158	-97.1	108.7	-66.3	85.1	30.8	23.6	4.65	0
159	-66.9	-28.8	-74.1	107.4	7.2	136.2	4.7	0
160	-64.3	-34.9	-72.4	147.9	8.1	177.2	6.99	9.85
161	-51.1	-34.8	-135.8	109.8	84.7	144.6	0	0
162	116.5	-0.9	-70.8	-0.9	172.7	0	0	0

DSSP files for 2HMG and 1HTM are aligned along their common residues, conformational angles  $\phi_{\rm pre}$ ,  $\psi_{\rm pre}$  prefusion and  $\phi_{\rm post}$ ,  $\psi_{\rm post}$  postfusion are given, and differences  $\Delta\phi$  and  $\Delta\psi$  are computed. The maximum of the  $\Pi$ -values of the two prospective BHBs are reported  $\Pi_{\rm pre}$  pre- and  $\Pi_{\rm post}$  postfusion.

Table 2. Conformationally Active and Exotic Residues in Test Cases

Viral Glycoprotein	#Residues	#Further Than One Away From Active	#Active	#One Away from Active	#Exotic
influenza glycoprotein HA chain F	122	70	33	19	7
paramyxovirus glycoprotein F chain A	422	81	251	90	62
tick-borne encephalitis glycoprotein E chain A	376	120	148	108	34
vesicular stomatitis glycoprotein G chain A	409	140	138	131	72

Displayed are the data upon which the *p*-values in SM Table 3 are based. For each virus, the pre- and postfusion PDB files are aligned in order to compare the change of conformational angles during reconformation. # Residues is the number of residues common to the aligned pre- and postfusion conformation PDB files, and # Exotic is the number of exotic prefusion residues, namely the number of predictions to be made.

Table 3. Distance d to nearest active residue for exotic residues

Viral Glycoprotein	d = 0	d = 1	d = 2	d > 2	First p-value	$\begin{array}{c} \mathbf{Second} \\ \mathbf{p-value} \end{array}$
influenza glycoprotein HA2 chain F	2/1	2/1	0/0	0/1	$\boxed{6.2\times10^{-3}}$	$2.8 \times 10^{-2}$
paramyxovirus glycoprotein F chain A	27/15	6/8	1/1	3/1	$\boxed{2.3\times10^{-2}}$	$7.2\times10^{-2}$
tick-borne encephalitits glycoprotein E chain A	7/7	2/9	0/5	2/2	$2.3 \times 10^{-4}$	$1.2\times10^{-1}$
vesicular stomatitis glycoprotein G chain A	17/4	12/15	2/10	3/9	$4.8\times10^{-1}$	$\boxed{4.8\times10^{-3}}$

Results presented as dissipative/conservative. p-values computed for the trinomial distribution discussed before. The first p-value tests significance of the implication: if a residue is exotic prefusion, then it is at most one residue away from an active residue, and for the second p-value all conservative results are discarded. Vesicular stomatitis is exceptional because its glycoprotein G can oscillate between pre- and postfusion conformations evidently with conserved exotic residues.

### Influenza Virus Type A Glycoprotein HA Prefusion (2HMG)

### Chain E

 $90.94\%\ 116/111\ 241/170\ 258/121\ 16/F136\ 256/150\ 86/57\ 158/160\ 221/227$   $95.98\%\ 284/286\ 288/50\ 150/72\ 253/181\ 65/61\ 308/293\ 114/109\ 304/F62\ 135/153\ 157/194\ 137/146\ 142/144$   $99\%\ F15/17\ 161/157\ F24/16\ 74/68$ 

 $100\%\ 19/F21\ 20/F14\ 29/31\ 95/63\ 106/102\ 124/255\ 147/136\ 198/195\ 207/209\ 254/152\ F63/303$ 

### Chain F

90-94% E16/136 36/24 101/96 **9/5** 95-98% 130/126 99% **15/E17 24/E16** 

100% E19/21 E20/14 10/4 11/5 63/E303 134/137 175/172

### †Influenza Virus Type A Glycoprotein HA Postfusion (1HTM)

### Chain F

90-94% 128/123 61/56 92/87 95-98% 63/59 107/103 134/137 50/45 99% 132/139 100% 44/40 57/52 108/102 160/157

### Paramyxovirus Glycoprotein F Prefusion (2B9B)

### Chain A

 $90-94\%\ 259/272\ 170/166\ 241/237\ 408/424\ 269/263\ 334/39\ 295/301\ 294/367\ 98/95\ 423/411\ 362/300\ 352/348$   $95-98\%\ 38/329\ 313/315\ 422/B106\ 354/351\ 328/330\ 297/299$   $99\%\ 258/219\ 373/375\ 300/296\ 262/270\ 491/486\ 24/21\ 441/437$ 

 $100\%\ 26/22\ 92/87\ 94/91\ 95/90\ 96/90\ 160/156\ 188/184\ 189/184\ 264/268\ 353/347\ 374/B114\ 376/372\ 416/418\ 419/415$ 

### Chain B

 $90-94\% \ \mathbf{132/127} \ 167/150 \ 68/65 \ 483/478 \ 300/296 \ 296/401 \ 357/353 \ 269/263135/130 \ 449/445 \ 258/219 \ \mathbf{129/124} \ 496/491 \ 390/412 \ 181/60 \ 70/66 \ 313/315 \ 408/424 \ 377/405$ 

95-98% 334/39 31/25 **374/C114 113/109** 376/372387/414 82/77 492/487 **A422/106** 145/141 315/312 297/299 319/339 99% 388/392 93/88 90/85 262/270 188/184

100% 27/23 46/275 92/87 95/90235/231 236/231 264/268 328/330 393/387 416/418 A374/114

### Chain C

 $90-94\%\ 484/479\ 271/261\ 29/25\ 384/379\ 416/418\ 220/257\ 377/405\ 373/37526/23\ 38/329\ 313/315\ 170/166\ 411/407\ 300/296\ 258/219\ 296/401\ 319/339\ 353/347$ 

95-98% 297/299 387/414 95/89 157/159 31/25 269/263 94/91

 $99\%269/263\ 94/91\ 328/330\ 473/469$ 

100% 96/90 102/96 113/109 188/184 189/184 264/268 278/43 388/392 393/387 408/424 485/480

# $\dagger$ Paramyxovirus Glycoprotein F Postfusion (1ZTM)

### Chain A

 $90-94\% \ \text{C}59/443\ 323/319\ 29/25\ 261/257\ 210/205\ 264/281\ 326/346\ 408/404\ 158/153\ 262/256\ 361/358\ 366/363\ 271/275\ \text{C}53/438\ 193/189$   $215/210\ 244/240\ 243/239$ 

95-98% B 229/219 254/249 84/79 423/425 395/399 289/38 363/359 229/C 219 303/408 363/359 229/C 219 303/408 363/359 363/35

99% 360/354 167/162 185/179 307/303448/445 353/349 469/464 460/456 63/59

 $100\%\ 30/26\ 31/25\ 38/336\ 155/150\ 166/161\ 199/194\ 216/211\ 235/231\ 242/238\ 320/322\ 354/349\ 380/382\ 421/427\ 470/465$ 

### Chain B

 $90-94\%\ 53/\text{C}438\ 88/83\ 191/186\ 426/422\ 174/169\ 276/270\ 303/408\ 264/28195/90\ 462/457\ \text{C}229/219\ 395/399\ 184/178271/275\ 234/230\ 95-98\%\ 229/\text{A}219\ 215/210\ 233/228\ 380/382\ 320/322\ 187/182\ 87/83\ 421/427$ 

 $99\%\ 423/425\ 335/337\ 38/336\ 366/363\ 172/167\ 262/256361/358$ 

 $100\%\ 31/25\ 83/7984/79\ 84/80\ 185/179\ 196/192\ 197/192\ 244/240\ 305/405\ 327/315\ 383/379\ 484/479$ 

### Chain C

 $90-94\% \ B53/438 \ 59/A44329/25 \ 301/374 \ 155/150 \ 42/340 \ 235/231 \ 31/25 \ 83/79 \ 463/458 \ 233/228 \ 271/275 \ 151/146 \ 229/B219 \ 53/A438 \ 476/472 \ 283/45 \ 383/380 \ 408/404326/346$ 

 $95\text{-}98\% \ 328/344 \ 30/26 \ 26/22 \ 203/198 \ 387/375 \ 185/179 \ 184/178$ 

99% 380/382 474/469 149/144 472/467

 $100\%\ 38/336\ 95/90\ 148/143\ 244/240\ 264/281\ 303/408\ 320/322\ 332/328\ 360/354\ 361/358\ 363/359\ 394/421\ 421/427\ 470/465$ 

Donor/Acceptor residues of BHBs in order of non-decreasing Π-values with 7.5, 8.5, 9.5 and 9.85 respectively corresponding to percentiles 90, 95, 99 and 100. Marked in boldface are the residues lying in generally agreed upon fusion loops. † indicates that the fusion loop is missing from the structure and therefore a fortiori contains no exotic BHBs.

### Tick-Borne Encephalitis Virus Glycoprotein E Prefusion (1SVB)

### Chain A

 $90-94\%\ 218/196\ 188/289\ 386/388\ 330/316\ 389/385\ 65/120\ 177/180\ 308/339\ 322/325\ 339/364\ 355/344$   $95-98\%\ 167/169\ 278/280\ 184/293380/394\ 372/148\ 388/309$   $99\%\ 366/368\ 360/373$ 

### Tick-Borne Encephalitis Virus Glycoprotein E Postfusion (1URZ)

### Chain A

 $90-94\%\ 258/241\ 28/286\ 29/45\ 380/394\ 218/196\ 278/280\ 181/177\ 388/309\ 317/329\ 355/344\ 78/74\ \mathbf{106/100}\ 360/373$   $95-98\%\ 249/251\ 389/385147/40\ 330/316$   $99\%\ 322/325\ 180/176\ 243/238\ 366/368\ 371/363\ 15/18\ 9/302$   $100\%\ 16/B13\ 167/169\ 177/180\ 192/285\ 251/248\ 252/248\ C16/13$ 

### Vesicular Stomatitis Virus Glycoprotein G Prefusion (5I2S)

### Chain A

 $90-94\%\ 224/226\ 313/262\ 332/6\ 320/322\ 185/43\ 314/328\ 37/33\ 324/403\ 9/329\ 55/134\ 183/45\ 136/144\ 372/316\ 150/159\ 16/325\ 345/342\ 298/400$   $95-98\%\ 104/98\ 333/208\ 38/190\ 51/47$ 

 $99\%\ 323/319\ 254/220\ 370/373\ 355/345\ 367/363\ 142/137\ 33/29\ 312/330\ 208/210$   $100\%\ 138/142\ 146/151152/148\ 261/234\ 348/352\ 351/347\ 359/10\ 364/366\ 404/321$ 

### Vesicular Stomatitis Virus Glycoprotein G Postfusion (5I2M)

### Chain A

 $90-94\%~\mathbf{72/75}~332/6~\mathbf{119/115}~254/220~225/138~377/379~258/254~261/234~216/203~219/215~38/190$   $95-98\%~312/330~374/370~\mathbf{71/118}~34/29~153/149~404/261$  99%~348/352~15/12~138/142~146/151~152/148~208/210 100%~105/98~364/366~370/373

Donor/Acceptor residues of BHBs in order of non-decreasing  $\Pi$ -values with 7.5, 8.5, 9.5 and 9.85 respectively corresponding to percentiles 90, 95, 99 and 100. Marked in boldface are the residues lying in generally agreed upon fusion loops.

### Bourbon Virus Glycoprotein Env Postfusion (5ZKX)

### Chain A

 $90 - 94\% \ 189/185 \ 117/93 \ 168/171 \ 140/97 \ 144/121 \ 109/105 \ 155/254 \ 239/241 \ 98/139 \ 145/48 \ 445/127$ 95-98% 253/271 358/341 **68/57** 101/137 99% 348/351 414/240 9/5  $100\%\ 44/148\ \mathbf{103/135}\ 106/101\ 116/93\ 238/207\ 349/351$ 

### Chikugunkya Virus Glycoprotein E1-E2-E3 Prefusion (3N41)

### Chain A

90-94% 18/6 95-98% 99% 100% 13/10

### Chain B

90-94% 58/61 245/F58 44/154 158/260 334/330 237/170 96/102 150/268 109/131 196/192 189/217 236/11 130/109 116/123  $95\text{-}98\% \ 31/17 \ 27/23 \ 16/51 \ 55/98 \ 75/71$ 99% 240/237 99/54 280/282 98/100

 $100\%\ 23/26\ 72/74\ 74/71\ 88/89\ 92/85\ 118/120\ 166/163\ 185/187\ 200/209\ 283/279\ 300/304\ F258/301$ 

### Chain F

 $90.94\%\ 160/156\ 157/159\ 252/184\ 109/74\ 370/372\ 125/175\ 373/369\ 381/361\ 248/243\ 203/199\ \textbf{85/100}\ 102/61\ 77/73\ \textbf{89/91}\ 60/103$ 95-98% 323/348 263/267 382/306 273/257 321/350 138/140 129/39 99% 315/356 88/227

 $100\% \ \mathbf{101/98} \ 151/163 \ 161/281 \ 258/B301 \ 268/262$ 

### Dengue Virus Glycoprotein E-M Prefusion (3J2P)

 $90-94\%\ 405/400\ 390/378\ 382/336\ 242/249\ 263/258\ 187/284\ \textbf{74/112}\ 86/82\ 430/427\ 366/363\ 468/463\ 349/339\ 119/66\ 61/219\ 181/291\ 22/287$  $95-98\%\ 412/407\ 443/438\ 335/300\ 411/406\ 250/241\ 41/38\ 189/186\ 252/239\ 410/405\ 180/175\ 286/23\ 433/428\ 190/186\ 330/327\ 233/220\ 447/441$ 163/139 78/75 341/377 50/136

99% 488/482 120/89 176/179 484/479 280/277 463/458 481/476 394/374 492/487 136/132 216/212 346/343 433/429 490/485  $100\%\ 9/6\ 21/16\ 29/26\ 62/123\ 79/76\ 87/83\ 91/87\ \textbf{104/100}\ \textbf{106/101}\ 126/59\ 156/153\ 179/175\ 182/173\ 183/288\ 199/128\ 202/204\ 215/211$  $262/257\ 265/261\ 277/272\ 284/25\ 287/184\ 290/19\ 308/325\ 321/369\ 326/307\ 328/305\ 345/342\ 395/373\ 396/373\ 398/395\ 400/396\ 401/396$  $404/399\ 408/403\ 413/408\ 415/412\ 416/411\ 420/416\ 421/417\ 434/429\ 434/428\ 435/430\ 436/431\ 439/434\ 447/443\ 448/444\ 451/9\ 461/456$  $469/464\ 475/472\ 477/473\ 479/475\ 483/479\ 489/484\ 493/489\ 493/488\ 494/489$ 

### Chain B

 $90\text{-}94\% \ 49/45 \ 48/43 \ 54/49 \ 52/47$ 95-98% 99% 51/46 31/26 46/41  $100\% \ 35/30 \ 53/48 \ 59/56 \ 60/56 \ 68/63 \ 71/66$ 

# Dengue Virus Glycoprotein E Postfusion (10K8)

 $90-94\%\ 284/25\ 161/141\ 298/6\ 392/376\ 382/336\ 334/358\ 245/247\ 363/326\ 303/334\ 119/66\ 202/204\ 354/368\ \mathbf{106/100}$ 95-98% 324/310 179/175 342/345 99% 166/168 316/319 274/276 37/293 $100\%\ 15/18\ 176/179\ 180/175\ 239/234\ 268/264\ 375/393\ 386/383\ 387/383$ 

# Dhori Virus Glycoprotein G<sub>p</sub> Postfusion (5XEB)

90-94% 188/191 160/117 **121/157** 94/71 175/281 118/159 95-98% 32/29 64/168 99% 164/141

Donor/Acceptor residues of BHBs in order of non-decreasing II-values with 7.5, 8.5, 9.5 and 9.85 respectively corresponding to percentiles 90, 95, 99 and 100. Marked in boldface are the residues lying in generally agreed upon fusion loops.

# Eastern Equine Encephalitis Virus Glycoprotein E1-E2 and Capsid C-terminal Prefusion (6MX4) Chain A

 $90-94\%\ 280/5\ 182/184\ 55/52\ 120/48\ 310/382\ 330/345\ 171/168\ 78/75\ 123/178\ 218/203\ 319/303\ 60/103\ 256/251\ 6/1\ 118/113\ 255/251\ 306/316$   $95-98\%\ 65/99\ 328/347\ 253/185\ 162/282\ 282/3\ 424/419\ 302/320\ 315/312\ 271/261\ B337/389\ 322/351$ 

99% 259/B298 84/98 257/252 201/197

 $100\%\ 4/281\ 4/2\ 14/11\ 18/15\ 77/73\ 88/228\ 89/91\ 105/79\ 141/137\ 142/137\ 146/133\ 153/150\ 184/181\ 185/181\ 230/226\ 244/239\ 246/242\ 316/357\ 356/317\ 371/373\ 389/386\ 412/408\ 416/411\ 422/417$ 

### Chain B

 $90-94\%\ 373/368\ 28/25\ 243/A58\ 249/246\ 230/227\ 411/408\ \mathbf{96/98}\ 33/29\ 77/65\ 381/376\ 201/222\ 319/278\ 42/151\ 180/186\ 279/276\ 285/312\ 225/198\ \mathbf{94/100}\ 404/400\ 358/353\ 182/184$ 

 $95\text{-}98\%\ 234/11\ 25/22\ 73/69\ 104/43\ 282/274\ 315/282\ 14/233\ 180/177\ 337/A389$ 

 $99\%\ 195/228\ \mathbf{90/83}\ 280/276\ 160/157\ 241/237$ 

 $100\% \ 16/50 \ 18/29 \ 23/25 \ 24/21 \ 57/60 \ 65/54 \ 65/61 \ 70/72 \ 75/67 \ \textbf{82/78} \ \textbf{86/87} \ 151/148 \ 198/206 \ 235/167 \ 255/162 \ 277/279 \ 293/306 \ 297/301 \ 370/365 \ 403/400 \ 251/396$ 

### Chain C

 $90-94\%\ 246/249\ 229/240\ 185/182\ 107/102\ 242/253\ 118/142\ 138/160\ 124/116\ 122/118\ 189/191\ 225/216$   $95-98\%\ 131/174\ 234/236\ 187/193\ 119/121$  90%

 $100\%\ 133/130\ 143/117\ 157/161\ 161/156\ 162/156\ 215/211\ 230/240\ 235/236\ 240/200\ 251/B396$ 

### Ebola Virus Glycoprotein GP Prefusion (5JQ3)

### Chain A

 $90.94\%\ 186/36\ 100/164\ 115/143\ 71/178\ 160/179\ 266/260\ 43/39\ 477/276\ 173/123$   $95.98\%\ 40/42\ 226/144\ 144/112\ 133/175\ 238/240\ 475/274\ 145/222$   $99\%\ 237/240\ 192/189\ 101/65$   $100\%\ 111/139\ 174/111\ B511/73$ 

### Chain B

90-94% **531/527** 95-98% 599/594 622/617 555/551 99% 628/623 100% 511/A73

### \*Epstein-Barr Virus Glycoprotein gp350 Prefusion (2H6O)

### Chain A

 $90-94\%\ 197/218\ 193/190\ 83/62\ 405/351\ 227/245\ 420/403\ 54/124\ 148/16\ 249/261\ 142/10\ 55/57\ 47/66\ 101/313\ 128/51\ 362/357\ 135/138$   $235/19\ 121/117\ 272/177\ 80/64\ 422/401\ 15/143\ 279/303$ 

 $95\text{-}98\%\ 385/388\ 397/394\ 208/204\ 17/145\ 334/389\ 432/428\ 210/202\ 33/30\ 260/257\ 86/112$ 

99% 176/178 46/133 389/385 223/220

 $100\%\ 44/41\ 58/54\ 73/69\ 74/69\ 98/101\ 194/191\ 195/192\ 209/23\ 234/210\ 243/267\ 277/273\ 314/311\ 339/336\ 355/38$ 

# Hanta Virus Glycoprotein $G_c$ Postfusion with scFv A5 (5LJY)

### Chain A

 $90.94\%\ 216/224\ 336/411\ 222/239\ 162/164\ 313/310\ 361/398\ 45/19\ 22/44\ 318/315\ 388/368\ 364/366\ 319/314\ 290/287\ \textbf{253/250}\ 95-98\%\ 293/285\ 63/33\ 379/349\ \textbf{95/91}\ 301/298\ 179/181\ 227/223\ 396/408\ 99\%\ 46/51\ 50/47$ 

 $100\%\ 74/229\ 288/290\ 335/340\ 337/388\ 412/333$ 

# $\textbf{Hanta Virus Glycoprotein} \ G_c \ \textbf{Postfusion} \ (5LJZ)$

### Chain A

90-94% 336/411 162/164 361/398 288/290 400/402 379/349 378/353 174/185 388/368 79/137 274/270 222/239 **127/113** 316/17 95-98% 240/219 216/224 63/33 175/171 364/366 315/179 99% 229/236 412/333 227/223 100% 74/229 179/181 205/202 **253/118** 335/340 396/408

Donor/Acceptor residues of BHBs in order of non-decreasing  $\Pi$ -values with 7.5, 8.5, 9.5 and 9.85 respectively corresponding to percentiles 90, 95, 99 and 100. Marked in boldface are the residues lying in generally agreed upon fusion loops. \* indicates a glycoprotein other than the fusion peptide which does not and is not expected to contain the fusion loop.

### \*Hendra Virus Glycoprotein G Receptor Bound (2VSK)

### Chain A

 $90-94\%\ 453/445\ 490/529\ 232/251\ 226/228\ 409/370\ 481/466\ 190/598\ 535/556\ 463/497\ 572/568\ 410/399\ 291/287\ 465/485\ 293/285\ 375/371\ 359/361\ 480/477\ 269/252\ 371/408\ 528/534\ 496/529$ 

 $95 - 98\%\ 385/382\ 589/215\ 558/581\ 352/365\ 432/411\ 413/366\ 521/515\ 316/295\ 542/544\ 194/546\ 484/542\ 257/264$ 

 $99\%\ 471/476\ 515/520\ 265/256\ 288/290\ 520/516\ 391/387$ 

 $100\%\ 245/237\ 255/266\ 345/342\ 347/369\ 362/358\ 368/349\ 376/372\ 440/409\ 448/450\ 477/471\ 507/122\ 516/520\ 562/508\ 569/571$ 

### Chain B

90-94% 103/81 102/81 46/42 69/107 95-98% 51/46

99% 130/118 80/104 44/41133/167

100% 47/50 79/143 99/95

### Hendra Virus Glycoprotein F Prefusion (5EJB)

### Chain A

 $90-94\%\ 320/322\ 321/290\ 293/318\ 224/221\ 439/435\ 396/419\ 307/303\ 197/192\ 361/358\ 262/256\ 42/295\ 184/178\ 415/430\ 285/50\ 235/231\ 283/53\ 46/336\ 271/275\ 70/66\ \mathbf{123/120}\ 323/319\ 384/412$ 

 $95\text{-}98\% \ 304/306 \ 276/270 \ 335/337 \ 326/346 \ 450/365 \ 431/381 \ 301/374 \ 30/356 \ 303/408$ 

99% 82/77

 $100\%\ 166/163\ 238/232\ 264/281\ 360/354\ 373/370\ 383/379\ 395/399\ 417/413\ 418/413\ 425/422\ 477/472$ 

### HIV Glycoprotein gp41 Prefusion (6MTJ)

### Chain E

90-94% 583/578 627/622 95-98% **532/623 543/538** 624/619

100% 531/626

### Influenza Virus D Glycoprotein HEF Prefusion (5E64)

### Chain A

 $90-94\%\ 155/103\ 382/399\ 44/367\ 278/127\ 356/359\ 34/414\ 393/406\ 130/277\ 407/390\ 82/53\ B75/402\ 305/155\ 288/210\ 41/384\ 378/385\ 17/27\ 221/307\ 248/260\ 295/246\ 106/152\ 54/79\ 159/302\ 22/B101\ 403/B74$ 

95-98% 182/93 425/24 215/217 193/199 200/192 38/391 B25/10

 $99\% \ \mathrm{B}18/11 \ 69/65 \ 72/58$ 

 $100\%\ 12/B15\ 70/65\ 122/327\ 127/174\ 173/178\ 178/172\ 179/175\ 205/293\ 261/247\ 270/231\ 312/148\ 342/B77\ 354/357\ 355/359\ 358/C28\ 374/370\ 382/397\ 404/377\ 358/C28$ 

### Chain B

 $90\text{-}94\%\ 145/142\ 75/\mathrm{A}402\ \mathrm{A}22/102\ \mathrm{A}403/74$ 

95-98% 48/45 **25/10** 

99% 18/A11

100% **16/A9** 40/29 135/138 **A12/15** A342/77

### Chain C

 $90-94\% \ 82/53 \ 183/93 \ 250/258 \ 288/210 \ 9/\mathrm{D}26 \ 295/246 \ 72/58 \ 305/155 \ 155/103 \ 205/293 \ 41/384 \ 130/277 \ 215/217 \ 179/175 \ 200/192 \ 22/\mathrm{D}102 \ 106/152$ 

 $99\%\ 278/127\ 70/65$ 

 $100\%\ 12/\mathrm{D}15\ 109/50\ 122/327\ 173/178\ 182/93\ 274/270\ 312/148\ 12/\mathrm{D}15$ 

# Chain D

90-94% C9/26

95-98%

99%

# \*Lassa Fever Virus Glycoprotein GP1 Receptor Bound (4ZJF)

### Chain B

 $\begin{array}{c} 90\text{-}94\%\ 202/214\ 87/231\ 103/225\ 169/218\ 197/191\\ 95\text{-}98\%\ 216/170\ 156/117\\ 99\%\ 162/158\ 211/207\ 99/101\\ 100\%\ 199/79\ 97/228 \end{array}$ 

Donor/Acceptor residues of BHBs in order of non-decreasing Π-values with 7.5, 8.5, 9.5 and 9.85 respectively corresponding to percentiles 90, 95, 99 and 100. Marked in boldface are the residues lying in generally agreed upon fusion loops. \* indicates a glycoprotein other than the fusion peptide which does not and is not expected to contain the fusion loop.

### Lymphatic Choriomeningitis Virus Glycoprotein GPC Prefusion (5INE)

### Chain A

 $90-94\%\ 311/306\ \mathbf{298/286}\ 104/106\ 74/379\ 248/244\ 233/166\ \mathbf{293/78}\ 368/362\ 166/162\ 69/72\ 391/376\ 382/71\ 161/122\ 95-98\%\ 381/385$ 

99% 201/196 401/393 168/161

100% 73/68 96/98 105/85 162/167 208/364 210/365 249/244 300/283 348/343 396/398

### Measles Virus Glycoprotein F Prefusion (5YXW)

### Chain A

 $\begin{array}{l} 90\text{-}94\% \ 74/\text{B}343 \ 69/65 \\ 95\text{-}98\% \ \text{B}280/56 \ 53/\text{B}283 \ 27/\text{B}359 \\ 99\% \end{array}$ 

100% 102/B115 B286/49

### Chain F

 $90.94\% \ A47/343 \ 230/267 \ 307/309 \ 444/409 \ 241/235 \ 232/265 \ 274/278 \ 326/322 \ 188/182 \ 398/402 \ \mathbf{126/123}$   $95.98\% \ 418/433 \ 383/385 \ 338/335 \ 280/A56 \ 187/182 \ 363/357 \ 235/230 \ 53/283 \ 27/359 \ 338/340 \ 310/306$   $99\% \ 323/325 \ 279/273 \ 400/422$   $100\% \ 286/49 \ 295/291 \ 329/349 \ 373/370 \ 434/384 \ \mathbf{A102/115}$ 

### \*Measles Virus Glycoprotein H Receptor Bound (3ALX)

### Chain A

 $90-94\%\ 595/592\ 601/579\ 98/106\ 359/291\ 388/383\ 40/138\ 262/269\ 486/496\ 574/576\ 387/382\ 444/355\ 552/542\ 37/334\ 455/468\ 213/208\ 392/388\ 411/430\ 315/312\ 273/203$ 

 $95\text{-}98\%\ 106/45\ 593/590\ 111/41\ 77/66\ 232/220\ 427/414\ 338/319\ 548/544\ 115/111\ 44/107$ 

 $99\%\ 274/257\ 307/349\ 365/357\ 383/378\ 472/477\ 225/227\ 125/127\ 86/83\ 592/589\ 460/463\ 75/72\ 441/438$ 

 $100\%\ 54/51\ 104/99\ 117/135\ 204/270\ 214/210\ 215/209\ 229/258\ 287/301\ 293/295\ 313/310\ 357/289\ 463/459\ 464/459\ 478/471\ 482/467\ 493/489\ 494/491\ 499/483\ 518/523\ 588/591$ 

### MERS Virus Spike Glycoprotein Prefusion Conformation 1 (5X5C)

### Chain A

 $90-94\% \ 981/976 \ 440/576 \ 59/278 \ 169/185 \ 91/300 \ 506/514 \ 934/803 \ 1152/778 \ 1036/1031 \ 493/391 \ 302/208 \ 329/332 \ 256/266 \ 148/171 \\ 400/396 \ 273/268 \ 280/267 \ 325/337 \ 297/146 \ 824/819 \ 1032/1027 \ 246/178 \ 991/987 \ 215/210 \ 1143/786 \ 343/696 \ 305/93 \ 1037/1031 \ 198/190 \ 454/450 \\ 539/558 \ 384/408 \ 399/395 \ 292/150$ 

 $95-98\% \ 913/908 \ 94/96 \ 1125/1139 \ 522/470 \ 907/676 \ 301/88 \ 320/75 \ 54/50 \ 127/123 \ 108/104 \ 185/239 \ 76/319 \ 113/291 \ 133/130 \ 674/660 \ 508/512 \ 939/936 \ 1181/1178 \ 669/664 \ 1137/793 \ 375/372 \ 372/604 \ 584/581 \ 1035/1030 \ 117/256 \ 392/490 \ 164/154$ 

 $99\%\ 1109/1103\ 1131/1133\ 857/854\ 370/688\ 1192/1189\ 855/850\ 1042/1037\ 970/779\ 809/805$ 

 $100\% \ 131/136 \ 175/179 \ 179/174 \ 180/174 \ 187/235 \ 195/199 \ 214/209 \ 337/50 \ 354/351 \ 375/605 \ 376/597 \ 389/385 \ 408/583 \ 470/464 \ 519/466 \ 551/546 \ 552/546 \ 599/596 \ 609/611 \ 651/618 \ 670/664 \ 741/761 \ 759/721 \ 765/762 \ 773/859 \ 798/795 \ 799/796 \ 808/810 \ 870/866 \ 986/983 \ 987/984 \ 1020/1016 \ 1107/1102 \ 1118/1114 \ 1146/1143 \ 1157/1203 \ 1158/1159 \ 1167/1192 \ 1173/1177$ 

# MERS Virus Spike Glycoprotein Prefusion Conformation 2 (5X5F)

### Chain A

 $90.94\% \ 981/976 \ 351/346 \ 59/278 \ 169/185 \ 320/75 \ 91/300 \ 506/514 \ 934/803 \ 1152/778 \ 1036/1031 \ 493/391 \ 302/208 \ 329/332 \ 256/266 \ 478/426 \\ 148/171 \ 400/396 \ 273/268 \ 280/267 \ 297/146 \ 824/819 \ 1032/1027 \ 246/178 \ 522/470 \ 991/987 \ 215/210 \ 1143/786 \ 305/93 \ 1037/1031 \ 198/190 \ 113/291 \\ 407/583 \ 454/450 \ 539/558 \ 384/408 \ 399/395 \ 292/150$ 

 $95-98\%\ 347/342\ 913/908\ 94/96\ 1125/1139\ 907/C676\ 80/48\ 301/88\ 54/50\ 127/123\ 108/104\ 185/239\ 133/130\ 674/660\ 508/512\ 939/936\ 1181/1178$   $669/664\ 1137/793\ 375/372\ 372/604\ 1035/1030\ 117/256\ 392/490\ 164/154$ 

 $99\%\ 1109/1103\ 857/854\ 370/688\ 1192/1189\ 855/850\ 1042/1037\ 585/438\ 970/C779\ 809/805$ 

 $100\%\ 131/136\ 175/179\ 179/174\ 180/174\ 187/235\ 195/199\ 214/209$ 

 $337/50\ 353/348\ 375/605\ 376/597\ 389/385\ 470/464\ 519/466\ 551/546\ 552/546\ 584/439\ 599/596\ 609/611\ 651/618\ 670/664\ 741/761\ 759/721\ 765/762\ 773/B859\ 798/795\ 799/796\ 808/810\ 870/866\ 986/983\ 987/984\ 1020/1016\ 1107/1102\ 1118/1114\ 1131/1133\ 1146/1143\ 1157/1203\ 1158/1159\ 1167/1192\ 1173/1177$ 

Donor/Acceptor residues of BHBs in order of non-decreasing II-values with 7.5, 8.5, 9.5 and 9.85 respectively corresponding to percentiles 90, 95, 99 and 100. \* indicates a glycoprotein other than the fusion peptide which does not and is not expected to contain the fusion loop. For 5X5C and 5X5F, the expected fusion loop is part of the structure at resides 880-900 but contains no exotic residues.

### \*MERS Virus Spike Glycoprotein Receptor Bound (4L72)

### Chain A

 $90-94\%\ 466/462\ 575/541\ 492/489\ 592/\ 587\ 621/540\ 668/663\ 687/683\ 572/567\ 649/624\ 303/314\ 580/525\ 509/41\ 104/117\ 585/552$ 485/489 214/197 545/625 654/628 633/629 76/72

 $95 - 98\% \ 523/519 \ 109/113 \ 541/618 \ 739/735 \ 137/141 \ 318/322 \ 405/382 \ 463/467 \ 412/414 \ 477/453 \ 308/310 \ 629/651 \ 430/455 \ 153/130 \ 456/474 \ 470/453 \ 470$ 355/320 520/522

99% 260/662 210/204 159/163 307/310 332/336 455/450 322/319 195/190 262/258

 $100\% \ 64/67 \ 65/67 \ 81/85 \ 124/127 \ 191/194 \ 197/170 \ 209/203 \ 218/222 \ 344/340 \ 366/370 \ 378/381 \ 426/422 \ 436/441 \ 458/429 \ 464/64 \ 489/484 \ 489/$ 552/582 558/427 560/473 574/567 583/ 590 597/670 624/620 680/673 681/675

90-94% 498/561 508/512 440/576 401/445 503/557 95-98% 522/470 468/463 470/464

100% 408/583 416/411 417/411 519/466 552/546 584/581

### Metapneumovirus Glycoprotein F Prefusion (5WB0)

### Chain F

 $90 - 94 \% \ 264 / 266 \ 313 / 282 \ 380 / 376 \ 393 / 401 \ 62 / 180 \ 309 / 286 \ 174 / 168 \ 29 / 24 \ 257 / 272 \ 418 / 393 \ 413 / 378 \ 281 / 37 \ 262 / 268 \ 338 / 40 \ 314 / 316$  $214/210\ 284/35\ 407/384\ 39/333\ 30/24\ 434/19\ 175/169$ 

95-98% 43/275 333/329 310/320 330/332 373/383 389/385 417/393

99% 377/379

100% 25/29 167/51 443/26

### †Metapneumovirus Glycoprotein F Postfusion (5L1X)

90-94% 48/D433 B334/36 79/74 88/B260 B284/35 95-98% B281/37 B279/39 30/24 66/63 99% 25/29 100% 36/B283 39/B333

90-94% 334/A36 421/423 258/214 220/F208 413/378 174/168 394/417 454/451 284/A35 407/384 309/286 218/252 373/383  $95 - 98\% \ 302/366 \ 314/316 \ 354/349 \ 281/A37 \ 303/291 \ 155/150 \ 175/169 \ 279/A39 \ 213/207 \ 251/247 \ 303/291 \ 303$ 99% 252/247 372/F315 158/153

100% 264/266 333/329 377/379 417/393 A36/283 A39/333 D372/315

### \*Mumps Virus Glycoprotein HN Prefusion (5B2C)

### Chain A

 $90\text{-}94\%\ 323/378\ 385/316\ 259/242\ 179/198\ 483/541\ 409/307\ 315/317\ 518/529\ 197/180\ 211/235$  $95-98\%\ 561/573\ 304/325\ 375/326\ 231/214\ 308/321\ 549/553\ 138/217\ 301/297\ 395/295\ 572/562\ 137/189\ B168/171$ 99% 569/174 391/386

 $100\% \ 168/B171 \ 221/224 \ 250/252 \ 283/286 \ 310/408 \ 406/375 \ 411/310 \ 417/413 \ 455/452 \ 462/509 \ 468/509 \ 542/480 \ 548/143 \ 548/14$ 

# Human Corona Virus Spike Glycoprotein Prefusion (5108)

### Chain A

 $90.94\%\ 427/367\ 82/240\ 1132/1146\ 650/B55\ 272/275\ 1146/799\ 720/692\ 807/1139\ 215/199\ 434/431\ 716/718\ 805/802\ 402/398\ 660/646$  $671/632\ 678/306\ 462/459\ 1114/1109\ 413/408\ 581/455\ 99/233\ 283/280\ 1131/1146\ 606/354\ 768/741\ 137/151\ 263/67\ 463/574\ 262/101$  $1115/1109\ 814/942\ 78/256\ 583/585\ 200/214\ 72/40\ 221/48\ 613/318\ 341/437$ 

 $95-98\%\ 1000/995\ 234/127\ 1001/996\ 626/319\ 1052/B832\ 1062/1058\ 117/114\ 695/717\ 690/680\ 745/736\ 826/822\ 1007/1002\ 661/665\ 158/18$ 320/623 88/26 205/100 823/820 742/B949 345/341 328/353 112/118

 $99\%\ 828/823\ 396/579\ 1138/1140\ 291/286\ 79/256\ 941/936$ 

 $100\%\ 17/156\ 47/218\ 55/51\ 59/271\ 95/91\ 96/91\ 109/196\ 143/145\ 146/142\ 230/207\ 280/43\ 375/B1064\ 414/408\ 415/409\ 416/409\ 449/444$  $586/582\ 600/626\ 605/381\ 621/631\ 651/654\ 728/764\ 739/742\ 767/729\ 817/813\ 827/823\ 927/923\ 937/932\ 973/968\ 1061/1057\ 1116/1110$ 

Donor/Acceptor residues of BHBs in order of non-decreasing  $\Pi$ -values with 7.5, 8.5, 9.5 and 9.85 respectively corresponding to percentiles 90, 95, 99 and 100. Marked in boldface are the residues lying in generally agreed upon fusion loops. \* indicates a glycoprotein other than the fusion peptide which does not and is not expected to contain the fusion loop. Part of the fusion loop is missing from 5L1X, and the residues 100-125 presumed to lie in the fusion loop a fortiori do not appear in exotic BHBs; in 5WB0 which contains the fusion loop, there is a bond with sub-exotic II-value 6.6, roughly the 82nd percentile, for a BHB with residues 112/109 in the fusion loop. † indicates that the fusion loop, though part of the peptide, is either missing from the the structure or disordered and in either case a fortiori can provide no reliable exotic BHBs. For coronavirus, the putative fusion loop at residues (I or L)EDLLF is controversial, disordered in 6B3O and contains no exotic BHBs in 5I08.

### †Murine Corona Virus Spike Glycoprotein Postfusion (6B3O)

### Chain A

 $90.94\%\ 1235/1231\ 750/1125\ 805/800\ 1153/1149\ 776/773\ 800/796\ 1176/B755\ C1176/755\ 1143/1170\ 1175/1138$   $95.98\%\ 1134/1137\ 1165/1155\ 1122/754\ 767/1108\ 1085/1079\ 1236/1231\ 1121/754$   $99\%\ 1208/1203\ 755/1121\ 1110/1106$   $100\%\ 782/776\ 1092/1096\ 1107/1109\ 1150/1152\ 1159/1143\ 1181/757\ 1200/780\ C1181/757\ C1200/780$ 

# $*Newcastle\ Virus\ Glycoprotein\ HN\ Prefusion\ Complexed\ With\ Thiosialoside\ (1USX)$

### Chain A

 $90-94\%\ 473/527\ 276/247\ 223/210\ 225/208\ 554/551\ 253/236\ 378/384\ 205/229\ 547/559\ 539/535\ 405/304\ 298/319\ 178/188\ 560/546\ 133/129\ 285/272\ 436/432\ 292/287\ 535/539\ 162/159\ 249/241\ 136/132$ 

95-98% 182/184 452/495 428/413 528/470 130/211 129/183 B217/230

 $99\%\ 456/452\ 555/169\ 540/534\ 368/364\ 408/410\ 215/218\ 550/523\ 505/489\ 294/290\ 275/282$ 

 $100\%\ 456/452\ 555/169\ 540/534\ 368/364\ 408/410\ 215/218\ 550/523\ 505/489\ 294/290\ 275/282$ 

### \*Newcastle Virus Glycoprotein HN Prefusion (3T1E)

### Chain A

 $90-94\%\ 301/314\ 408/137\ 136/132\ 311/307\ 319/296\ 472/526\ 276/279\ 210/221\ 451/494\ 457/494\ 377/383\ 274/281\ 561/543\ 236/251\ 142/475\ 479/482\ 517/500\ 491/501\ 493/499\ 133/129$ 

 $95-98\%\ 549/522\ 284/271\ 474/487\ 190/174\ 305/239\ 185/208\ 524/497\ 402/300\ 504/488\ 399/368\ 404/303\ 535/131\ 158/561$   $99\%\ 534/538\ 533/135\ 201/197\ 482/478$ 

 $100\%\ 180/185\ 182/183\ 186/179\ 197/192\ 243/245\ 303/401\ 364/360\ 396/391\ 455/451\ 507/509\ 539/533\ 550/553\ 554/549\ 555/B551\ B555/551$ 

### Chain B

 $90-94\%\ 402/300\ 545/527\ 527/469\ 377/383\ 136/132\ 444/423\ 305/239\ 185/208\ 372/315\ 319/296\ 426/441\ 214/217\ 533/135\ 485/476\ 301/314\ 474/487\ 201/197\ 243/245\ 197/193$ 

 $95\text{-}98\%\ 479/482\ 534/538\ 195/170\ 158/561\ 467/417\ 408/137\ 357/352\ 554/549\ 404/303$ 

 $99\%\ 432/434\ 523/548\ 435/431\ 451/494\ 504/488\ 134/130\ 327/323$ 

 $100\%\ 180/185\ 182/183\ 186/179\ 197/192\ 210/221\ 224/207\ 252/236\ 292/287\ 295/291\ 358/353\ 395/391\ 399/368\ 424/443\ 455/451\ 472/52657/509\ 536/131\ 539/533\ 550/553\ 555/A551\ A555/551$ 

### Chain E

90-94% 86/81 102/97 95-98% 99% 100% 89/85 98/93

# Chain F

 $\begin{array}{c} 90\text{-}94\% \\ 95\text{-}98\% \ 93/87 \\ 99\% \\ 100\% \ 86/82 \ 100/95 \ 104/99 \end{array}$ 

# †Newcastle Virus Glycoprotein F Postfusion (3MAW)

### Chain A

 $90-94\%\ 54/347\ 316/308\ 234/269\ 437/425\ 432/429\ 402/406\ 245/239\ 247/244\ 368/365\ 394/382\ 94/89\ 284/63$   $95-98\%\ 83/78\ 333/353\ 288/59\ 327/329\ 329/326$   $99\%\ 401/428\ 165/160\ 50/343\ 47/302\ 474/469\ 342/344\ 41/37$   $100\%\ 187/182\ 189/184\ 278/282\ 367/361\ 387/389$ 

Donor/Acceptor residues of BHBs in order of non-decreasing  $\Pi$ -values with 7.5, 8.5, 9.5 and 9.85 respectively corresponding to percentiles 90, 95, 99 and 100. Marked in boldface are the residues lying in generally agreed upon fusion loops. \* indicates a glycoprotein other than the fusion peptide which does not and is not expected to contain the fusion loop. † indicates that the fusion loop, though part of the peptide, is missing from the the structure or disordered and in either case a fortiori can provide no reliable BHBs. For coronavirus, the putative fusion loop at residues (I or L)EDLLF is controversial, disordered in 6B3O and contains no exotic BHBs in 5108.

### \*Nipah Virus Glycoprotein G Prefusion (2VWD)

### Chain A

 $90-94\% \ 297/280 \ 359/361 \ 226/228 \ 307/302 \ 235/218 \ 212/209 \ 311/307 \ 222/232 \ 357/363 \ 213/209 \ 385/382 \ 484/542 \ 521/515 \ 265/256 \ 433/475 \ 288/290 \ 569/571 \ 506/458$ 

 $95 - 98\% \ 194/546 \ 542/544 \ 481/466 \ 190/598 \ 413/366 \ 218/588 \ 562/508 \ 463/497 \\ 99\% \ 410/399 \ 269/252 \ 471/476 \ 515/520 \ 328/324 \ 270/252$ 

 $100\%\ 259/262\ 291/287\ 331/327\ 440/409\ 445/354\ 448/450\ 477/471\ 511/561\ 516/520$ 

### \*Nipah Virus Glycoprotein G Receptor Bound (2VSM)

### Chain A

 $90-94\%\ 297/280\ 307/302\ 359/361\ 545/541\ 385/382\ 235/218\ 445/354\ 357/363\ 481/466\ 451/447\ 269/252\ 288/290\ 490/529\ 245/237\ 291/28759/215\ 226/228\ 328/324\ 562/508\ 507/122$ 

 $95-98\%\ 484/542\ 542/544\ 347/369\ 463/497\ 432/411\ 569/571\ 413/366\ 440/409\ 194/546\ 511/561\ 215/586$   $99\%\ 259/262\ 410/399\ 471/476\ 332/327\ 515/520\ 190/598\ 448/450\ 483/480\ 516/520\ 472/476\ 477/471$  100%

### Chain B

90-94%51/46 133/167 59/117 103/81 69/107 162/155 102/81 79/143 80/104 170/166 95-98% 130/118 156/141 47/50 157/139 99% 100%

# \*Parainfluenza Type 5 Virus Glycoprotein HN Sialyllactose Soaked (1Z4X)

### Chain A

 $90-94\% \ 298/300 \ 414/440 \ 171/173 \ 553/160 \ 520/516 \ 445/492 \ 185/159 \ 436/415 \ 443/411 \ 214/197 \ 301/297 \ 525/463 \\ 95-98\% \ 362/305 \ 466/524 \ 552/157 \ 309/286 \ 461/407 \ 358/309 \ 351/356 \ 505/507 \ 269/265 \ 533/122 \ 424/426 \\ 99\% \ 480/472 \ 204/207 \ 356/350 \ 392/290 \ 531/126 \ 266/269 \ 537/531 \\ 100\% \ 120/172 \ 233/235 \ 293/391 \ 357/353 \ 389/358 \ 394/293 \ 398/128 \ 439/505 \ 449/445 \ 501/512 \ 548/552 \ 559/541$ 

### Pseudorabies Virus Glycoprotein B Postfusion (6ESC)

### Chain A

 $90.94\%\ 239/280\ 681/665\ 198/185\ 223/243\ 248/218\ 249/261\ 258/254\ 379/423\ 214/209\ 219/214\ 461/410\ 216/210\ 451/469\ 567/562\ 343/347\ 539/534\ 408/402\ 685/677\ 219/213\ 628/657\ 675/671\ 680/682\ 595/597\ 644/631$   $95-98\%\ 190/192\ 303/306\ 435/430\ 312/324\ 460/463\ 647/650\ 417/456$   $99\%\ 688/675\ 215/209\ 474/446\ 298/294\ 241/237\ 619/624\ 161/385\ 403/407\ 275/188$   $100\%\ 122/124\ 217/211\ 339/353\ 445/439\ 447/443\ 464/459\ 672/674$ 

# \*Puumala Virus Glycoprotein $G_n$ (5FXU)

### Chain A

 $90.94\%\ 138/115\ 224/252\ 190/192\ 369/335\ 335/139\ 74/133\ 134/71\ 45/263$   $95.98\%\ 321/310\ 182/34\ 243/238\ 143/145$   $99\%\ 57/144\ 116/76\ 118/137$   $100\%\ 46/154\ 198/377\ 211/378\ 291/371\ 323/363\ 352/141$ 

# Puumala Virus Glycoprotein $G_c$ Postfusion at pH 6.0 (5J81)

### Chain A

 $90.94\% \ 1057/1059 \ 737/795 \ 993/1068 \ \textbf{772/785} \ 837/839 \ 887/893 \ 831/811 \ 897/877 \ 823/819 \\ 95.98\% \ 945/947 \ 1036/1006 \ 885/881 \ 759/755 \ 880/896 \ 931/927 \ \textbf{785/771} \\ 99\% \ 1021/1023 \ 874/882 \ 721/691 \ 708/703 \\ 100\% \ 820/822 \ \textbf{910/776} \ 919/898 \ 992/997 \ 994/1045 \ 1035/1010 \ 1053/1065 \ 1069/990$ 

# Puumala Virus Glycoprotein $G_c$ Postfusion at pH 8.0 (5J9H)

### Chain A

 $90.94\% \ 973/675 \ 837/839 \ 975/673 \ 737/795 \ 822/819 \ 820/822 \ 889/891 \ 993/1068$   $95.98\% \ 931/927 \ 887/893 \ 1057/1059 \ 1069/990 \ 945/947 \ 1036/1006 \ \textbf{788/744} \ 1053/1065 \ 1060/1056$   $99\% \ 721/691 \ 874/882$   $100\% \ 704/709 \ 885/881 \ 992/997 \ 994/1045 \ 1021/1023$ 

Donor/Acceptor residues of BHBs in order of non-decreasing II-values with 7.5, 8.5, 9.5 and 9.85 respectively corresponding to percentiles 90, 95, 99 and 100. Marked in boldface are the residues lying in generally agreed upon fusion loops. \* indicates a glycoprotein other than the fusion peptide which does not and is not expected to contain the fusion loop.

### Respiratory Sphinctial Virus Glycoprotein F Prefusion at pH 5.5 (4MMS)

90-94% B320/37 B475/35 B311/46 86/81 34/38 61/B193 95-98% 51/B305 103/B241 B197/60 99% 62/B295

100% 48/B365 68/65

### Chain B

 $90-94\% \ 265/260 \ 267/264 \ 324/332 \ 320/A37 \ 439/416 \ 287/302 \ 248/282 \ 341/316 \ 484/479 \ 475/A35 \ 203/198 \ 311/A46 \ 479/475 \ A61/193 \ 398/487 \ A61/193 \ 398/487 \ A61/193 \ A61/1$ 373/369 405/415

 $95 - 98\%\ 365/361\ \mathbf{D408/144}\ A51/305\ 205/199\ 342/352\ 409/411\ F145/405\ 243/237\ A103/241\ 408/F144\ 197/A60$ 99% 346/348 A62/295

100% 145/D405 294/296 421/417 445/410 A48/365

# Respiratory Sphinctial Virus Glycoprotein F Prefusion at pH 9.5 (4MMR)

### Chain A

90-94%39/33 31/B465 93/89 B370/49 51/B305 38/33 B193/58 95-98% B314/44 99% B466/28 81/76 34/38 84/81 98/95

 $100\%\ 48/\mathrm{B}365\ 52/\mathrm{B}305\ 62/\mathrm{B}295\ 78/74\ 88/83\ 91/86\ \mathrm{B}306/51\ \mathrm{B}311/46$ 

### Chain B

 $90.94\%\ 338/394\ A31/465\ 497/492\ \textbf{150/146}\ 244/240\ 512/507\ 453/455\ 267/264\ 272/267\ 433/424\ 398/487\ 370/A49\ 182/185\ 341/316$ A51/305 364/361 193/A58 220/217 445/410 301/288 405/415 203/199 202/198  $95\text{-}98\% \ 399/333 \ 291/298 \ 449/425 \ 314/A44 \ 402/399 \ 475/A35 \ 345/312 \ 362/364 \ 188/179$ 99% 466/A28 308/305 346/348

 $100\%\ 173/169\ 297/293\ 306/A51\ 311/A46\ 373/369\ 409/411\ 431/426\ 506/501\ 508/503\ A48/365\ A52/305\ A62/295$ 

### †Respiratory Sphinctial Virus Glycoprotein F Postfusion (3RRR)

### Chain A

90-94% 62/B295 90/86 34/38 51/B305 D465/54 95-98% B308/48 99%

100% 39/33

### Chain B

 $90 - 94\,\% \ 362/364 \ 303/286 \ A62/295 \ 170/165 \ 186/181 \ 441/414 \ 459/E50 \ 436/422 \ 465/E54 \ 250/F238 \ A51/305 \ 450/425 \ 299/291$  $95 - 98\%\ 348/345\ 439/416\ 449/425\ 308/A48\ 205/199\ 433/424\ 499/494\ 341/316\ 457/F307$  $99\%\ 342/352\ 248/282\ 213/208\ 427/430\ 409/411\ 294/296\ 241/236\ 227/222\ 172/167\ 223/218\ 405/415\ 202/197\ 373/369\ 380/376\ 358/354/350$  $100\%\ 219/214\ 226/221\ 460/448$ 

# Rift Valley Fever Virus Glycoprotein $G_c$ Postfusion (6EGT)

### Chain A

 $90-94\%\ 893/1010\ 1116/1038\ 1113/1093\ \textbf{832/817}\ 1026/704\ 747/864\ 1059/1075\ 1008/724\ 813/793\ 1017/885\ 802/798\ 909/912\ 1115/1091$  $1026/C704\ 972/1122\ 1041/1115\ 854/757\ 857/755\ 1076/1058\ 866/869\ 932/928\ 986/988\ 785/782\ 764/934\ 810/943\ 784/780$ 95-98% 693/729 1019/1015 960/962 997/993 726/723

99% 946/807 826/820 884/886 855/757 737/741

 $100\%\ 718/1\ 018\ 780/783\ 788/784\ 821/827\ 899/C897\ 904/B900\ \mathbf{962/959}\ \mathbf{963/959}\ 994/998\ 1040/1045\ 1079/1054\ 1125/969\ C904/900$ 

# Rubella Virus Glycoprotein E1 Postfusion (4ADI)

# Chain A

 $90 - 94\% \ 67/62 \ 49/142 \ \textbf{89/139} \ 238/39 \ 107/103 \ 169/25 \ 327/3 \ 384/362 \ 79/147 \ \textbf{123/86} \ 140/88 \ 149/42 \ 32/161 \ 157/207 \ 286/131 \ 123/100 \ 140/100 \$  $95\text{-}98\% \ 35/351 \ 91/97 \ 289/279 \ 312/307 \ 349/411 \ 357/389$ 99% 351/413 324/195 273/294

 $100\%\ 16/21\ 22/15\ 110/101\ 172/174\ 180/182\ 188/190\ 248/297\ 282/129\ C248/297$ 

Donor/Acceptor residues of BHBs in order of non-decreasing  $\Pi$ -values with 7.5, 8.5, 9.5 and 9.85 respectively corresponding to percentiles 90, 95, 99 and 100. Marked in boldface are the residues lying in generally agreed upon fusion loops. † indicates that the fusion loop, though part of the peptide, is missing from the the structure or disordered and in either case a fortiori can provide no reliable BHBs.

### SARS Virus Spike Glycoprotein Prefusion Conformation 1 (5X58)

### Chain A

 $90 - 94\% \ 286/281 \ 937/932 \ 562/552 \ 1015/1010 \ 184/91 \ 554/47 \ 1039/1036 \ 259/59 \ 89/255 \ 1033/1047 \ 94/181 \ 420/499 \ 981/976 \ 985/980$  $1047/705\ 68/254\ 658/677\ 239/246\ 261/57\ 702/1050\ 256/88\ 423/363\ 597/584\ 599/582\ 725/720\ 363/422\ 452/411\ 133/130\ 370/367\ 615/609$  $443/477\ 680/655\ 496/423\ 335/332\ 1079/1085\ 656/846\ 879/865\ 162/127\ 476/460\ 740/736$ 

 $95-98\%\ 235/100\ 932/927\ 350/321\ 636/599\ 461/475\ 43/216\ 565/569\ 116/126\ 240/140\ 1042/1038\ 726/721\ 299/585\ 621/280\ 230/104\ 431/425$ 60/258 82/231 561/552 869/866

 $99\%\ 115/103\ 510/379\ 120/122\ 655/845\ 676/659\ 64/35\ 129/113\ 480/440\ 330/325\ 579/576\ 924/919\ 73/75\ 293/287\ 146/141$  $100\%\ 51/267\ 223/194\ 226/192\ 379/530\ 392/490\ 398/393\ 454/225\ 507/504\ 526/536\ 530/532\ 635/631\ 674/661\ 754/749\ 765/760\ \textbf{780/782}$ **783/779** 868/862 931/927 1016/1010 1017/1011 1039/1041 1056/696 1083/1080

### SARS Virus Spike Glycoprotein Prefusion Conformation 2 (5X5B)

### Chain A

 $90-94\%\ 120/122\ 859/854\ 657/653\ 696/B877\ B48/551\ 872/868\ 643/676\ \textbf{783/779}\ 420/499\ 561/552\ 562/552\ 82/231\ 261/57\ 528/525$  $289/284\ 423/363\ 1083/1080\ 363/422\ 268/271\ 452/411\ 1033/1047\ 952/B737\ 939/935\ 370/367\ 949/945\ 553/550\ \textbf{778/775}\ 1060/692\ 443/477$  $804/799\ 496/423\ 100/234\ 335/332\ 526/536\ 615/612\ 932/927\ 67/33\ 569/564\ 867/862\ 324/349\ 476/460$ 

 $95 - 98\% \,\, \mathrm{B}50/553 \,\, 937/932 \,\, 621/280 \,\, 461/475 \,\, 223/194 \,\, 315/376 \,\, \textbf{780/782} \,\, 733/728 \,\, 293/287 \,\, 674/661 \,\, 1072/1103 \,\, 431/425 \,\, 632/634 \,\, 331/232 \,\,$  $99\%\ 736/731\ 879/865\ 975/970\ 480/440\ 609/604\ 553/561\ 924/919\ 162/127\ 330/325\ 599/582\ 735/731\ 146/141$ 

 $100\%\ 39/35\ 43/216\ 48/C551\ 51/267\ 54/264\ 115/103\ 129/113\ 185/199\ 200/184\ 239/246\ 240/140\ 258/86\ 264/276\ 314/376\ 392/490\ 398/393$  $530/532\ 555/556\ 579/576\ 582/303\ 597/584\ 635/631\ 741/738\ 754/749\ 765/760\ 805/800\ 868/862\ 869/866\ 873/868\ 892/887\ 931/927\ 972/966$ 1017/1011 1042/1038 1056/696

### †SARS Virus Spike Glycoprotein Receptor Bound (2AJF)

### Chain A

 $90 - 94\% \ 207/203 \ 107/103 \ 42/37 \ 97/92 \ 461/456 \ 55/341 \ 536/530 \ 393/389 \ 263/486 \ 216/212 \ 156/151 \ 352/355 \ 348/345 \ 366/363 \ 564/560 \ 344/51 \ 366/360 \ 344/51 \ 344/51 \ 34$  $95 - 98\% \ 488/481 \ 44/39 \ 331/326 \ 125/120 \ 218/209 \ 153/148 \ 284/279 \ 361/332 \ 507/503 \ 280/276 \ 174/168$ 

99% 341/338 563/392 293/290 560/555 40/35 210/217 603/599

 $100\%\ 25/20\ 71/66\ 135/140\ 149/146\ 149/143\ 150/146\ 150/144\ 170/165\ 197/191\ 276/444\ 333/358\ 363/333\ 425/418\ 447/442\ 449/443\ 467/462$ 479/474 487/481 511/505 559/554

### Chain E

90-94% 430/425 389/335 356/352 421/365 394/390 95-98% 452/411 411/405 357/352 447/444 431/426 449/407 99% 407/403 472/468 100% 393/490 408/403

### Semliki Forest Virus Glycoprotein E1 Postfusion (1RER)

### Chain A

 $90.94\% \ 321/350 \ 53/109 \ 31/136 \ 160/156 \ 157/159 \ 181/183 \ 21/286 \ 10/274 \ 261/269 \ 327/346 \ 366/376 \ 128/39 \ 370/372 \ \mathbf{104/59} \ 47/121 \ 20/27 \ \mathbf{104/59} \ \mathbf{104/59}$  $95\text{-}98\%\ 271/36\ 263/267\ 77/73\ \mathbf{100/97}\ 274/271\ 167/147\ 217/202\ \mathbf{85/100}\ \mathbf{92/89}$ 

99% 28/19 315/356 308/313 33/134 24/21 314/310 255/251 316/305

 $100\%\ 45/309\ \mathbf{102/62}\ 138/140\ 141/137\ 190/187\ 203/199\ 254/250\ 256/251\ 259/340\ 260/256\ 268/262\ 392/389$ 

# Sindbis Virus Glycoprotein E1-E2 Prefusion (3MUU)

### Chain A

 $90 - 94\% \ 332/294 \ 605/600 \ 368/636 \ 525/637 \ 53/63 \ 299/327 \ \mathbf{444/460} \ 583/592 \ 286/317 \ 597/577 \ 155/262 \ 329/336 \ 64/60 \ 510/523 \ 424/421 \ 13/48 \ 329/336 \ 64/60 \ 510/523 \ 424/421 \ 13/48 \ 329/336 \ 64/60 \ 510/523 \ 424/421 \ 13/48 \ 329/336 \ 64/60 \ 510/523 \ 424/421 \ 13/48 \ 329/336 \ 64/60 \ 510/523 \ 424/421 \ 13/48 \ 329/336 \ 64/60 \ 510/523 \ 424/421 \ 13/48 \ 329/336 \ 64/60 \ 510/523 \ 424/421 \ 13/48 \ 329/336 \ 64/60 \ 510/523 \ 424/421 \ 13/48 \ 329/336 \ 64/60 \ 510/523 \ 424/421 \ 13/48 \ 424/421 \ 13/4$ 612/544 563/559 621/629 314/289

 $95 - 98\% \ 131/108 \ 61/52 \ 327/338 \ 287/275 \ 402/485 \ 484/403 \ 608/603 \ 105/92 \ 45/35 \ 623/627 \ 374/370 \ 276/286 \ 23/627 \ 23/6$ 

 $99\%\ 588/585\ 95/102\ 489/399\ 385/381\ \textbf{452/449}\ 437/433\ 40/153$ 

 $100\%\ 20/21\ 54/63\ 98/100\ 100/97\ 101/97\ 263/154\ 280/282\ 290/313\ 300/304\ 322/281\ 324/321\ 337/334\ 380/387\ 432/429\ 472/410\ 517/514$ 

# Thogoto Virus Glycoprotein G<sub>p</sub> Prefusion (5XEA)

90-94% 46/221 258/260 177/173 32/412 150/73 83/72 116/153 184/187 120/116 132/108 202/204 156/112 160/137 180/19195-98% 71/84 176/173

99% 174/176 74/150 87/68 243/222

100% 171/258 261/257 292/186

Donor/Acceptor residues of BHBs in order of non-decreasing II-values with 7.5, 8.5, 9.5 and 9.85 respectively corresponding to percentiles 90, 95, 99 and 100. Marked in boldface are the residues lying in generally agreed upon fusion loops. † indicates that the fusion loop, though part of the peptide, is missing from the the structure or disordered and in either case a fortiori can provide no reliable BHBs.

# Table 5. (continued) Exotic BHB Donor/Acceptor Residues of Viral Glycoproteins

### West Nile Virus Glycoprotein E Prefusion (2HG0)

### Chain A

 $90.94\%\ 127/124\ 129/203\ 297/183\ 338/303\ 392/388\ 280/50\ 358/374\ 353/342\ 306/337\ 383/397\ 139/47\ 262/258\ 266/262\ 181/184\ 186/294\ 52/134\ 146/143\ 163/159\ 205/211$ 

95-98% 177/188 319/322 276/278 144/163 154/150 185/181  $\mathbf{106/100}$ 

 $99\%\ 114/95\ 369/329\ 267/263\ 279/275\ 30/26$ 

 $100\%\ 48/138\ 57/127\ 72/114\ 74/112\ 86/82\ 171/173\ 202/198\ 209/206\ 210/206\ 220/215\ 239/235\ 244/241\ 264/259\ 270/266\ 354/342\ 373/147\ 381/399\ 393/388\ 400/380$ 

# Yellow Fever Virus Glycoprotein E Prefusion (6IW4)

### Chain A

 $99.94\% \ \mathbf{98/111} \ 63/123 \ 251/61 \ 248/231 \ 349/368 \ 202/198 \ 373/391 \ 292/175 \ 119/66 \ \mathbf{112/97} \ 180/286 \\ 95-98\% \ 352/366 \ 347/336 \ 265/202 \ 302/299 \ 148/145 \ 364/322 \\ 99\% \ \mathbf{106/103} \ 192/187 \ 361/324 \ 7/3 \\ 100\% \ 173/176 \ 178/289 \ 314/317$ 

### Yellow Fever Virus Glycoprotein E Postfusion (6IW1)

### Chain A

 $90.94\%\ 144/155\ B19/11\ 119/66\ 123/62\ 361/324\ 7/32\ 120/89\ 351/366\ 183/166\ 127/197\ 373/391\ 177/172\ 352/366$   $95.98\%\ 19/C11\ 331/356\ 202/198\ 301/331\ 199/201\ 239/241\ 63/123$   $99\%\ 173/176\ 296/6\ 205/262$   $100\%\ 14/B16\ 15/18\ 16/C13\ 19/C8\ 163/165\ 165/133\ 221/56\ 314/317\ 347/336\ B16/13\ B19/8\ C14/16$ 

### Zika Virus Glycoprotein E Prefusion (6CO8)

### Chain A

 $90.94\%\ 340/337\ 179/186\ 205/211\ 500/496\ 216/200\ 323/320\ 290/25\ 31/8\ 17/20\ 295/187\ 389/344\ 221/217\ 51/282\ \textbf{114/95}\ 466/461\ 124/6292/117\ 207/209$ 

 $95\text{-}98\%\ 384/402\ 443/438\ 333/372\ 309/340\ 335/370\ 322/325\ 185/180\ 361/377\ 238/225\ 138/169$ 

99% 376/147 452/447 28/287 471/466

 $100\%\ 50/136\ \mathbf{112/97}\ 184/180\ 188/294\ 249/252\ 270/265\ 450/445\ 458/453\ 459/453\ 460/457\ B13/271$ 

### Chain B

90-94% 56/53 37/32 95-98% 99%

100% 13/A271

Donor/Acceptor residues of BHBs in order of non-decreasing II-values with 7.5, 8.5, 9.5 and 9.85 respectively corresponding to percentiles 90, 95, 99 and 100. Marked in boldface are the residues lying in generally agreed upon fusion loops. For yellow fever postfusion, the fusion loop is not missing from the structure and yet contains no exotic BHBs.

### Human Adenovirus 2 (1X9P)

### Chain A

 $90\text{-}94\%\ 464/439\ 227/285\ 183/178\ 263/424\ 237/212\ 474/516$ 

 $95-98\%\ 114/533\ 249/273\ 276/246\ 131/553\ 546/549\ 538/109\ 235/232\ 446/441\ 72/559\ 217/214\ 565/120\ 560/71\ 234/231\ 452/448\ 174/134$   $99\%\ 240/211\ 386/389\ 198/192\ 280/277\ 206/202$ 

 $100\% \ 53/49 \ 61/58 \ 123/562 \ 152/199 \ 182/178 \ 194/189 \ 195/190 \ 200/197 \ 201/197 \ 221/225 \ 230/226 \ 390/385 \ 395/400 \ 460/456 \ 471/468 \ 485/481 \ 549/545$ 

### Foot and Mouth Virus (1FOD)

### Chain 1

 $\begin{array}{c} 90\text{-}94\%\ 57/53\ 89/104\ 43/176\ 3\text{:}167/122\ 182/75\ 70/66 \\ 95\text{-}98\%\ 71/186\ 172/83\ 174/46\ 21/15\ 190/68\ 2\text{:}148/6\ 3\text{:}168/122 \\ 99\%\ 115/3\text{:}10\ 39/36\ 20/16\ 151/147 \\ 100\%\ 134/2\text{:}173\ 139/136\ 142/2\text{:}172 \end{array}$ 

### Chain 2

 $90\text{-}94\%\ 170/101\ 217/3\text{:}138\ 105/206\ 77/183\ 189/118\ 154/149\ 20/22$   $95\text{-}98\%\ 23/19\ 121/185\ 148/1\text{:}6$   $99\%\ 11/8\ 194/189$   $100\%\ 13/6\ 30/13\ 139/135\ 1\text{:}134/173\ 1\text{:}142/172}$ 

### Chain 3

90-94%57/85 2:217/138 54/203 80/182 100/213 167/1:122 50/45 97/92 81/78 126/143 95-98% 150/119 58/61 207/104 168/1:122 119/192 121/190 99% 1:115/10 197/66

100% 100/212 206/48 12/8

### Chain 4

90-94% 95-98% 99%

100% 70/65 70/66

### Hepatitis A Virus (5WTE)

### Chain A

 $90-94\%\ 267/\text{C}96\ 184/179\ 126/270\ 75/72\ 245/148\ 250/93\ 77/26\ 96/247\ 71/43\ 151/242\ 230/109\ 137/258\ 107/173\ 95-98\%\ 143/250\ 136/259\ 136/258\ 52/48\ B138/263\ 89/84\ 210/B166\ C30/201\ 99\%\ 129/124\ 224/219$ 

100% C27/199

### Chain B

 $\begin{array}{c} 90\text{-}94\%\ 171/104\ 218/100\ 124/188 \\ 95\text{-}98\%\ 138/A263\ C61/139\ 58/53\ 188/123 \\ 99\% \\ 100\%\ 30/13\ 76/186\ 103/214\ 151/154\ 210/107 \end{array}$ 

### Chain C

90-94% A267/96 54/50 202/136 139/199 88/61 75/71 245/86 208/130 229/55 95-98% 184/196 61/B139 91/95 30/A201 99% 83/80 74/206 69/218 100% 27/A199 47/43

99% 283/151 258/254 437/434 503/507 590/587 469/601 357/353

# ${\bf Hepatitis} \,\, {\bf E} \,\, {\bf Virus} \,\, (2{\rm ZTN})$

# Chain A Acceptors

 $90-94\%\ 144/298\ 172/320\ 156/278\ 286/203\ 313/181\ 341/332\ 424/418\ 432/331\ 532/534\ 437/327\ 324/440\ 500/474\ 600/471\ 581/570\ 392/219$   $252/248\ 261/270\ 567/564\ 373/439\ 328/436\ 603/540\ 397/371\ 354/446$ 

252/248 261/270 567/564 373/439 328/436 603/540 397/371 354/446 95-98% 141/300 178/173 393/220 374/394 408/405 132/308 195/242 378/149 487/484 451/447 333/340 287/291 273/268 351/346 507/502 515/510

 $100\%\ 142/166\ 199/297\ 203/199\ 315/312\ 323/169\ 330/434\ 338/334\ 361/358\ 364/360\ 393/388\ 395/390\ 396/390\ 449/351\ 485/482\ 522/524\ 573/578$ 

Donor/Acceptor residues of BHBs in order of non-decreasing  $\Pi$ -values with 7.5, 8.5, 9.5 and 9.85 respectively corresponding to percentile 90, 95, 99 and 100.

95-98% 99% 100%

```
Polio Virus (5O5B)
Chain 1
90\text{-}94\% \ 204/126 \ 194/3\text{:}22 \ 92/101 \ 163/159 \ 269/125
95\text{-}98\%\ 276/2\text{:}183\ 717/2\text{:}267\ 125/268\ 130/263
99% 134/259
100% 3:25/193
Chain 2
90-94% 37/33
107/209 235/121 175/133
95 - 98\% \ 3:125/116 \ 17/23 \ 1:276/183 \ 123/197 \ 1:217/267 \ 178/157 \ 144/171 \ 226/82 \ 103/218 \ 55/259
100\% 86/81 101/260 182/176 184/179 203/198
Chain 3
90\text{-}94\%\ 196/129\ 63/58\ 97/92\ 215/51\ 1\text{:}194/22
95\text{-}98\%\ 178/110\ 56/67\ 125/2\text{:}116\ 197/129\ 22/4\text{:}38
100\%\ 25/1{:}193\ 53/2{:}187\ 57/67\ 109/223
Chain 4
90-94%
95-98% 3:22/38
99%
100%
Rhinovirus (4AYM)
90 - 94\% \ 85/230 \ 76/238 \ 68/3:41 \ 120/241 \ 181/3:22 \ 189/2:207 \ 233/82 \ 236/125 \ 280/3:57 \ 3:25/180 \ 24/53 \ 114/110 \ 24/53 \ 24/53 \ 24/53 \ 24/53 \ 24/53 \ 24/53 \ 24/53 \ 24/53 \ 24/53 \ 24/53 \ 24/53 \ 24/53 \ 24/53 \ 24/53 \ 24/53 \ 24/53 \ 24/53 \ 24/53 \ 24/53 \ 24/53 \ 24/53 \ 24/53 \ 24/53 \ 24/53 \ 24/53 \ 24/53 \ 24/53 \ 24/53 \ 24/53 \ 24/53 \ 24/53 \ 24/53 \ 24/53 \ 24/53 \ 24/53 \ 24/53 \ 24/53 \ 24/53 \ 24/53 \ 24/53 \ 24/53 \ 24/53 \ 24/53 \ 24/53 \ 24/53 \ 24/53 \ 24/53 \ 24/53 \ 24/53 \ 24/53 \ 24/53 \ 24/53 \ 24/53 \ 24/53 \ 24/53 \ 24/53 \ 24/53 \ 24/53 \ 24/53 \ 24/53 \ 24/53 \ 24/53 \ 24/53 \ 24/53 \ 24/53 \ 24/53 \ 24/53 \ 24/53 \ 24/53 \ 24/53 \ 24/53 \ 24/53 \ 24/53 \ 24/53 \ 24/53 \ 24/53 \ 24/53 \ 24/53 \ 24/53 \ 24/53 \ 24/53 \ 24/53 \ 24/53 \ 24/53 \ 24/53 \ 24/53 \ 24/53 \ 24/53 \ 24/53 \ 24/53 \ 24/53 \ 24/53 \ 24/53 \ 24/53 \ 24/53 \ 24/53 \ 24/53 \ 24/53 \ 24/53 \ 24/53 \ 24/53 \ 24/53 \ 24/53 \ 24/53 \ 24/53 \ 24/53 \ 24/53 \ 24/53 \ 24/53 \ 24/53 \ 24/53 \ 24/53 \ 24/53 \ 24/53 \ 24/53 \ 24/53 \ 24/53 \ 24/53 \ 24/53 \ 24/53 \ 24/53 \ 24/53 \ 24/53 \ 24/53 \ 24/53 \ 24/53 \ 24/53 \ 24/53 \ 24/53 \ 24/53 \ 24/53 \ 24/53 \ 24/53 \ 24/53 \ 24/53 \ 24/53 \ 24/53 \ 24/53 \ 24/53 \ 24/53 \ 24/53 \ 24/53 \ 24/53 \ 24/53 \ 24/53 \ 24/53 \ 24/53 \ 24/53 \ 24/53 \ 24/53 \ 24/53 \ 24/53 \ 24/53 \ 24/53 \ 24/53 \ 24/53 \ 24/53 \ 24/53 \ 24/53 \ 24/53 \ 24/53 \ 24/53 \ 24/53 \ 24/53 \ 24/53 \ 24/53 \ 24/53 \ 24/53 \ 24/53 \ 24/53 \ 24/53 \ 24/53 \ 24/53 \ 24/53 \ 24/53 \ 24/53 \ 24/53 \ 24/53 \ 24/53 \ 24/53 \ 24/53 \ 24/53 \ 24/53 \ 24/53 \ 24/53 \ 24/53 \ 24/53 \ 24/53 \ 24/53 \ 24/53 \ 24/53 \ 24/53 \ 24/53 \ 24/53 \ 24/53 \ 24/53 \ 24/53 \ 24/53 \ 24/53 \ 24/53 \ 24/53 \ 24/53 \ 24/53 \ 24/53 \ 24/53 \ 24/53 \ 24/53 \ 24/53 \ 24/53 \ 24/53 \ 24/53 \ 24/53 \ 24/53 \ 24/53 \ 24/53 \ 24/53 \ 24/53 \ 24/53 \ 24/53 \ 24/53 \ 24/53 \ 24/53 \ 24/53 \ 24/53 \ 24/53 \ 24/53 \ 24/53 \ 24/53 \ 24/53 \ 24/53 \ 24/53 \ 24/53 \ 24/53 \ 24/53 \ 24/53 \ 24/53 \ 24/53 \ 24/53 \ 24/53 \ 2
95-98% 254/2:176 115/246 3:85/282
99\% \ 3{:}163/35 \ 2{:}75/15
100% 75/3:15 241/71
Chain 2
90.94\%\ 256/98\ 175/169\ 141/137\ 220/82\ 86/81\ 106/247\ 189/207\ 103/211\ 122/227\ 219/82\ 134/174\ 102/252\ 196/191\ 38/34\ 168/133\ 176/172
95\text{-}98\%\ 144/164\ 60/56
99% 94/89 228/121 190/1:38
100% 29/12 177/172 178/172 3:53/180
Chain 3
90\text{-}94\% 1:68/41 221/110 1:181/22 1:280/57 171/168 11/7 25/1:180
95\text{-}98\%\ 108/222\ 216/47\ 65/61\ 85/1:282\ 152/133
99\% 163/1:35 96/91 95/91 196/128
100\%\ 53/2{:}180\ 57/67\ 1{:}75/15
Chain 4
90-94% 29/3 4/28
```

Donor/Acceptor residues of BHBs in order of non-decreasing Π-values with 7.5, 8.5, 9.5 and 9.85 respectively corresponding to percentiles 90, 95, 99 and 100.

### References

- N. J. Dimmock, A. J. Easton, K. N. Leppard, Introduction to Modern Virology (Blackwell Publishing, 6th edition, 2007).
- [2] A. J. Levine, Viruses (Scientific American Library, 1992).
- [3] S. Shanker, S. Ramani, R. L. Atmar, M. K. Estes, B. V. Venkataram Prasad, Structural features of glycan recognition among viral pathogens. *Current Opinions in Structural Biology* 44, 211-218 (2017).
- [4] S. Boulant, M. Stanifer, P.-Y. Lozach, Dynamics of Virus-Receptor Interactions in Virus Binding, Signaling, and Endocytosis. Viruses 7(6), 2794-2815 (2015).
- [5] M. G. Rossman, Viral cell recognition and entry. Protein Science 3(10), 1712-1725 (1994).
- [6] L. V. Chernomordik, M. M. Kozlov, Mechanics of membrane fusion. *Nature Structural and Molecular Biology* 15(7), 675-683 (2009).
- [7] S. C. Harrison, Viral membrane fusion. Nature Structural Molecular Biology 15(7), 690-698 (2008).
- [8] J. A. Thorley, J. A. Keating, J. Z. Rappoport, Mechanisms of viral entry: sneaking in the front door. *Protoplasma* **244**, 15-24 (2010).
- [9] J. M. White, S. E. Delos, M. Brecher, K. Schomberg, Structures and mechanisms of viral membrane fusion proteins: multiple variations on a common theme. *Critical of reviews* in *Biochemistry and Molecular Biology* 43, 189-219 (2008). 2, 3, 4, 6
- [10] B. Tsai, Penetration of nonenveloped viruses into the cytoplasm. Annual Reviews Cellular and Developmental Biology 23, 23-43 (2007).
- [11] C. L. Moyer, G. R. Nemerow, Viral weapons of membrane destruction: variable modes of membrane penetration by non-enveloped viruses. *Current Opinions in Virology* 1(1), 44-49 (2011). 4
- [12] P. W. Choppin, A. Scheid, The Role of Viral Glycoproteins in Adsorption, Penetration, and Pathogenicity of Viruses. Reviews of Infectious Diseases 2(1), 40-61 (1980).
- [13] Viral Glycoprotein Structure, Viruses-Special Issue, editor A. Ward (2015).
- [14] A. V. Finkelstein, O. Ptitsyn, Protein Physics, A Course of Lectures (Academic Press, 2nd edition, 2016).
- [15] F. M. Pohl, Empirical protein energy maps. Nature New Biology 234, 277-279 (1971).
- [16] A. V. Finkelstein, A. M. Gutin, A. Ya Badretdinov, Boltzmann-like statistics of protein architectures: Origins and consequences. Sub-cellular Biochemistry 24, 1-26 (1995).
- [17] Finkelstein, A. Ya Badretdinov, A. M. Gutin, Why do protein architectures have Boltzmann-like statistics? *Proteins* 23, 142-150 (1995)
- [18] H. M. Berman, J. Westbrook, Z. Feng, G. Gilland, T. N. Bhat, H. Weissig, I. N. Shindyalov, P. E. Bourne, The Protein Data Bank. *Nucleic Acids Research* 28, 235-242 (2000).
- [19] R. C. Penner, E. S. Andersen, J. L. Ledet, A. K. Kantcheva, M. Bublitz, P. Nissen, A. M. H. Rasmussen, K. L. Svane, B. Hammer, R. Rezazadegan, N. C. Nielsen, J. T. Nielsen, J. E. Andersen, Hydrogen bond rotations as a uniform structural tool for analyzing protein architecture. *Nature Communications* 5, 5803 (2014). 1, 2
- [20] G. Wang, R. L. Dunbrack, Jr., PISCES: a protein sequence culling server. *Bioinformatics* 19.1589-1591 (2003).
- [21] W. Kabsch, C. Sander, DSSP: definition of secondary structure of proteins given a set of 3D coordinates. *Biopolymers* 22, 2577-2637 (1983).
- [22] T. Smith, M. S. Waterman, Identification of Common Molecular Subsequences. *Journal of Molecular Biology* 147(1), 195-197 (1981).
- [23] T. J. Tuthill, D. Bubeck, D. J. Rowlands, J. M. Hogle, Characterization of Early Steps in the Poliovirus Infection Process: Receptor-Decorated Liposomes Induce Conversion of the Virus to Membrane-Anchored Entry-Intermediate Particles. *Journal of Virology* 80(1), 172-180 (2006). 4
- [24] Y. He, V. D. Bowman, S. Mueller, C. M. Bator, J. Bella, X. Peng, T. S. Baker, E. Wimmer, R. J. Kuhn, M. G. Rossman, Interaction of the poliovirus receptor with poliovirus. Proceedings of the National Academy of Sciences 97(1), 79-84 (2000).
- [25] O. Carugo, How large B-factors can be in protein crystal structures? BMC Bioinformatics 19(61) (2018). 1